Chapter 2

Enhancing the Cellular Uptake of Pyrrole-Imidazole Polyamides Through Next-Generation Aryl Turns

The text of this chapter was taken in part from a manuscript co-authored with Jordan L. Meier and Peter B. Dervan (California Institute of Technology)

(Meier, J. L.; Montgomery, D. C.; Dervan, P. B. "Enhancing the cellular uptake of Py-Im polyamides through next-generation aryl turns" *Nucleic Acids Research* **2012**, 40 (5): 2345-2356)

Abstract

Pyrrole–imidazole (Py–Im) hairpin polyamides are a class of programmable, sequence-specific DNA binding oligomers capable of disrupting protein–DNA interactions and modulating gene expression in living cells. Methods to control the cellular uptake and nuclear localization of these compounds are essential to their application as molecular probes or therapeutic agents. Here, we explore modifications of the hairpin γ-aminobutyric acid turn unit as a means to enhance cellular uptake and biological activity. Remarkably, introduction of a simple aryl group at the turn potentiates the biological effects of a polyamide targeting the sequence 5′-WGWWCW-3′ (W = A/T) by up to two orders of magnitude. Confocal microscopy and quantitative flow cytometry analysis suggest this enhanced potency is due to increased nuclear uptake. Finally, we explore the generality of this approach and find that aryl-turn modifications enhance the uptake of all polyamides tested, while having a variable effect on the upper limit of polyamide nuclear accumulation. Overall this provides a step forward for controlling the intracellular concentration of Py–Im polyamides that will prove valuable for future applications in which biological potency is essential.

Introduction

Hairpin pyrrole-imidazole (Py-Im) polyamides are a class of heterocyclic amino acid oligomers that can be programmed to bind a wide repertoire of DNA sequences with high affinity and specificity.[1,2] Sequence-selective recognition of the minor groove of DNA is achieved through side-by-side stacked ring pairings: Im/Py distinguishes G·C from C·G, while Py/Py is degenerate for T·A and A·T. In recent years our group has focused on the biological evaluation of eight-ring polyamides arranged in a hairpin configuration through a γ-aminobutyric acid linker (Figure 2.1).[3,4] These compounds are of modest (~1300 Da) molecular weight and recognize 6 base pairs (bp) of DNA, similar to the size of many eukaryotic transcription factor binding sites.[5] When applied to living cells, hairpin polyamides can disrupt protein-DNA interactions and modulate the expression of genes induced by many transcription factors, including the ligand-activated nuclear receptors glucocorticoid receptor (GR) and androgen receptor (AR).[6-10] However, one persistent challenge encountered when applying Py-Im polyamides to new biological systems is cellular uptake. Previous studies have shown that the nuclear localization of fluorescently labelled polyamides can be influenced by several variables including molecular weight, modifications to the C-terminal moiety, and composition of Py/Im content.[11-13] In particular, Py-Im polyamides incorporating multiple (>2-3) *N*-methylimidazole subunits show reduced nuclear localization, limiting the ability to target GC rich sequences *in vivo*.[14] Therefore, new solutions for enhanced uptake are important for advancing Py-Im polyamides as probes of transcription factor binding and, potentially, as therapeutic agents.

While a large amount of work has been done one the effect of C-terminal modifications on polyamide nuclear localization,[13,15] relatively few studies have explored the impact of modifications to the γ-aminobutyric acid (GABA) turn moiety on biological activity. The incorporation of a chiral (R)-α-amino substituent on the GABA turn enforces polyamide binding in a N-terminus→C-terminus orientation with respect to the 5'→3' direction of the adjacent DNA strand.[16]

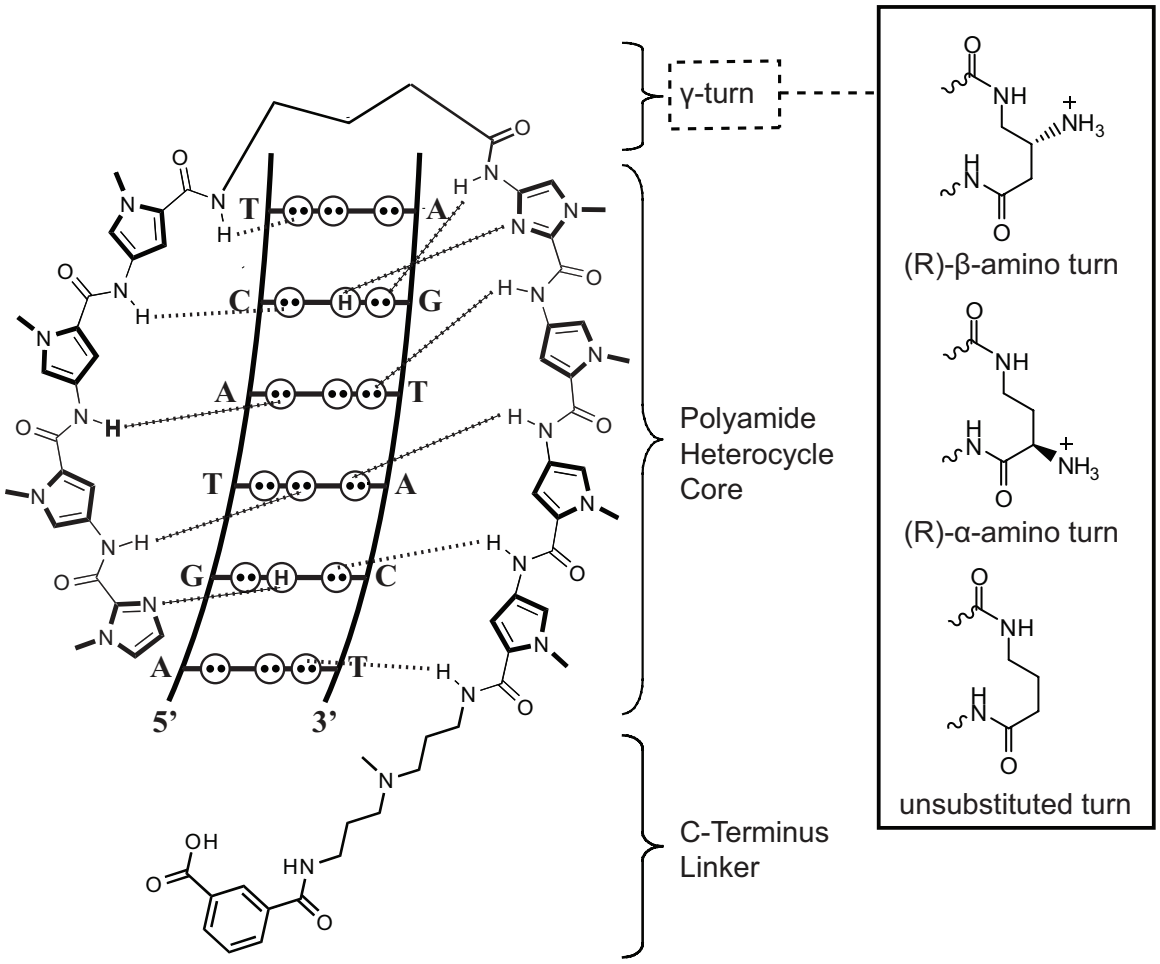

Figure 2.1: Schematic diagram of eight-ring Py–Im polyamides targeting the sequence 5' -WGWWCW-3' (W=A/T). Dashed lines indicate hydrogen bonds between the polyamide and DNA base pairs. The γ-aminobutyric acid turn unit enforces an antiparallel hairpin configuration, and codes for W.[16] Substitution of the chiral turn functionality can have substantial effects on DNA-binding and biological activity.

More recently, we introduced hairpin polyamides bearing (R)-β-amino GABA turns which show increased DNA-binding affinity and, importantly for the purposes of this study, a negligible decrease in DNA-binding affinity upon acylation (Figure 2.1).[16] Structural studies suggest this is due to their unique stereochemical presentation of the chiral β-amino moiety, which is directed up and out of the minor groove floor, thereby providing a chemical handle for introduction of functionality at the turn position.[17] Furthermore, biological evaluation of a β-acetylated polyamide targeted to the consensus androgen response element (ARE) half site 5'-WGWWCW-3' (W = A/T) showed inhibition of prostate specific antigen (PSA) gene expression at 10-fold lower concentrations relative to polyamides bearing unsubstituted β-amino turns, illustrating the ability of turn substitution to potentiate gene regulatory effects.[18]

Guided by these results, we explored modifications of the Py-Im polyamide hairpin γ-aminobutyric acid turn unit as a means to enhance uptake and biological activity. Our strategy applied cytotoxicity analysis at an extended time point as an effective assay for identifying biologically active polyamides from small focused libraries. This led to the discovery that for a hairpin polyamide targeting the DNA sequence 5'-WGWWCW-3' (W = A/T), simple conversion of the β-amino turn to a β-benzamide turn led to a 100-fold increase in gene regulatory activity. To better understand the mechanism of this phenomenon, fluorescent analogues of β-amino and β-aryl polyamides were synthesized and analyzed by confocal microscopy and quantitative flow cytometry. Our results suggest the enhanced potency of β-aryl polyamides is due to increased nuclear uptake of these compounds.

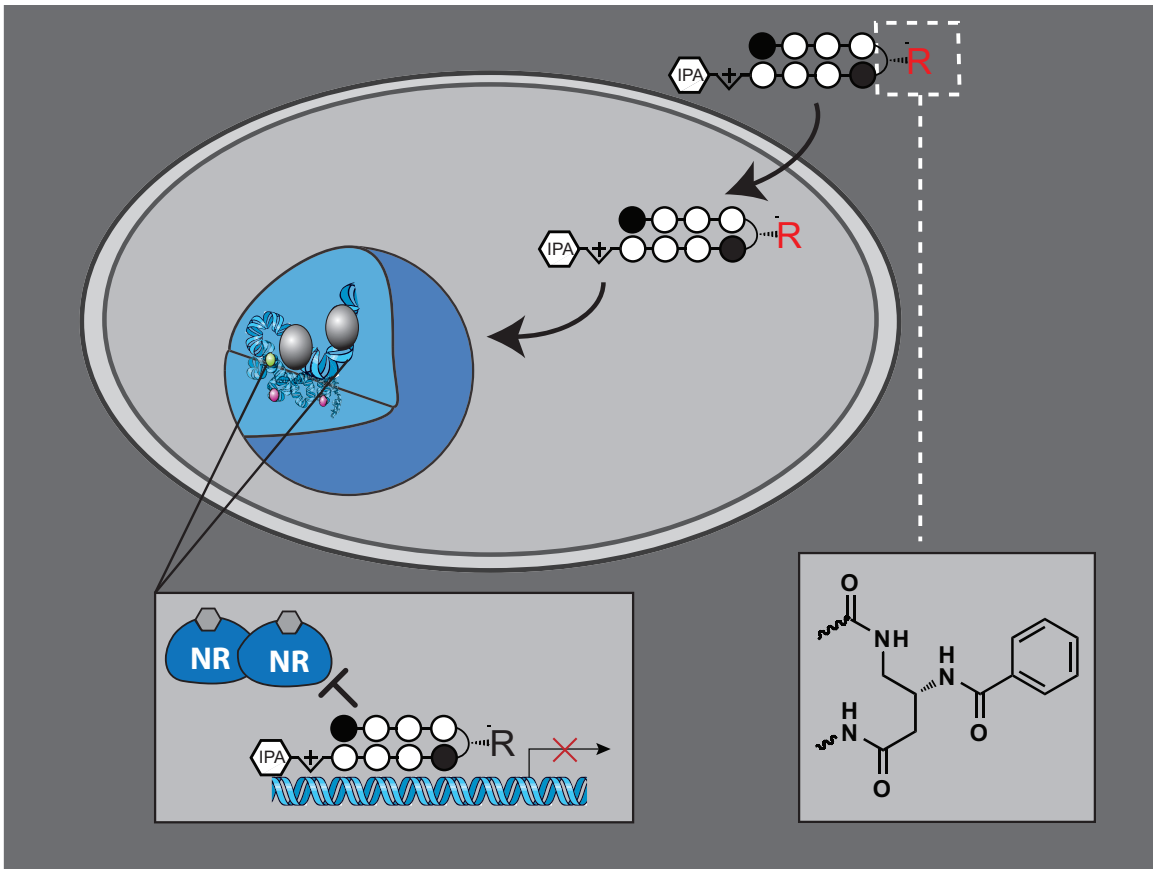

Figure 2.2: Based on a simple structural modification, pyrrole-imidazole polyamides have been developed with increased cellular uptake. This class of compounds can traffic to cell nuclei and access chromatin, imparting gene regulatory effects at lower concentrations.

Finally, we explore the generality of this modification and find that aryl-turn substitution capably enhances the uptake of other polyamides cores, but has a variable effect on the upper limits of polyamide nuclear accumulation. Overall this provides a new direction for controlling the intracellular concentration of Py-Im polyamides that will prove essential for future applications in which biological potency is required.

Results and Discussion

Synthesis, DNA-Binding, and Cytotoxicity of β-aryl Polyamides

Following an unanticipated observation that a hairpin polyamide conjugated to an aryl group at the β-amino position showed greater activity in cell culture, we synthesized a small panel of β-aryl substituted polyamides (**4**-**12**) targeting the sequence 5'-WGWWCW-3' and benchmark their DNA-binding affinities and biological activity against unsubstituted parent (**1**), β-amino (**2**), and β-acetylated (**3**) GABA turns in the A549 human lung carcinoma cell line (Figure 2.3). We used cytotoxicity at 96 hours as a proxy for uptake following the observation that polyamide uptake, gene regulatory activity, and cytotoxicity are often highly correlated.[13] Thermal denaturation analysis of a DNA duplex of the sequence 5'-TTGC**TGTTCT**GCAA-3' (polyamide match site in bold) shows all polyamides containing a β-amino GABA group (**2**-**14**) similarly increase the melting temperature by ~13-15 °C, suggesting no substantial energetic penalty for appendage of the bulky β-aryl groups (Figure 2.3). Cytotoxicity analyses demonstrate that β-amino GABA incorporating polyamide **2** (IC_{50} = 3.155 μM) is considerably more cytotoxic than its unsubstituted counterpart **1** (IC_{50} >30 μM). While this trend mirrors the relative duplex stabilization of these molecules (ΔT_m **1** = 8.8 °C; ΔT_m **2** = 13.3 °C), simple *N*-acetylation of the β-amino turn (**3**) results in another order of magnitude increase in growth inhibition while not greatly affecting binding affinity (ΔT_m **3** = 13.2 °C). Replacement of the acetyl unit of **3** with a benzoyl functionality (**4**) results in approximately another order of magnitude increase in cytotoxicity (IC_{50} = 35 nM), again without concomitant change in the duplex stabilizing ability of this minor groove binder. Within the aryl series (**4**-**12**) several trends are seen, including increased cytotoxicity of

p-substituted benzoic acids (compare **9** and **10**) and a preference for electron-withdrawing groups at the *p*-position (compare **6** and **7**). Remarkably, significantly increasing the steric bulk of the β-aryl turn, as in polyamides **8** and **11**, does not greatly affect either DNA-binding or cytotoxicity, arguing against interaction of the β-aryl turn with a small pocket of a specific protein partner as a mechanism of cytotoxicity.

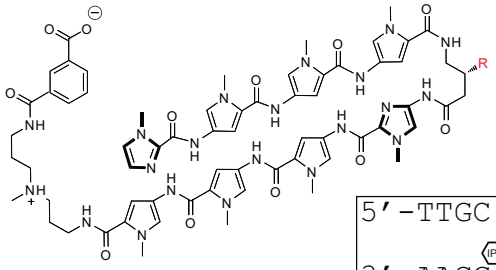

5′-TTGC **TGTTCT** GCAA-3′
3′-AACG **ACAAGA** CGTT-5′

R:	IC_{50} (nM)	ΔT_m / °C	R:	IC_{50} (nM)	ΔT_m / °C
1	> 30,000	8.8 ± 0.2	**7**	92 ± 38	14.0 ± 0.8
2	3200 ± 900	13.3 ± 0.6	**8**	13 ± 5	13.2 ± 0.9
3	180 ± 15	13.2 ± 0.1	**9**	37 ± 17	13.0 ± 1.1
4	35 ± 9	13.0 ± 0.9	**10**	200 ± 25	12.2 ± 1.7
5	21 ± 5	15.1 ± 0.6	**11**	85 ± 13	13.0 ± 0.7
6	10 ± 4	12.4 ± 0.6	**12**	190 ± 3	13.0 ± 0.5

Figure 2.3: Biological activity and DNA-binding of β-substituted hairpin polyamides. Cytotoxicity analyses were conducted 96 hr after polyamide treatment in the A549 lung carcinoma cell line. IC_{50} values represent the mean of three biological replicates. ΔT_m denotes the shift in melting temperature following polyamide treatment for the 5'-WGWWCW-3' duplex DNA sequence shown.

Since previous studies have noted that polyamide activity can be strongly influenced by cell type,[12] we tested the generality of the increased cytotoxicity of **4** and **9** in LNCaP prostate cancer, MCF-7 breast cancer, and HCT-116 colon cancer cell lines. All three cell lines showed a similar increase in potency for β-aryl compared to β-amino polyamides as was observed in A549 cells (Table 2.1).

	cell line			
Polyamide	A549	LNCaP	HCT-116	MCF-7
2	3155 ± 895	2550 ± 91	4680 ± 954	24400 ± 9530
4	35 ± 9	28 ± 12	106 ± 18	666 ± 168
9	37 ± 17	109 ± 19	136 ± 13	470 ± 77

Table 2.1: Cytotoxicity of β-amino (**2**) and β-aryl (**4**, **9**) polyamides targeting the sequence 5'-WGWWCW-3' towards alternative cancer cell lines. Growth inhibition values represent the mean and standard deviation of three biological replicates.

Suppression of Nuclear-Receptor Mediated Gene Expression by β-Aryl Polyamides

A549 lung epithelial cells have been widely applied as a model for inflammatory gene expression mediated by the transcription factor glucocorticoid receptor (GR).[23-25] GR is a member of larger family of nuclear receptors that utilize activation by small molecule ligands in order to affect release from cytoplasmic inhibitory complexes, after which they traffic to the nucleus, multimerize with their cognate protein partners, and activate (or repress) transcription (Figure 2.4A). Hairpin polyamides have been previously shown to inhibit nuclear receptor-DNA interactions in cell culture, making them promising agents for mechanistic studies of nuclear receptor-DNA binding and therapeutic modulation of nuclear receptor activity in diseases such as prostate cancer.

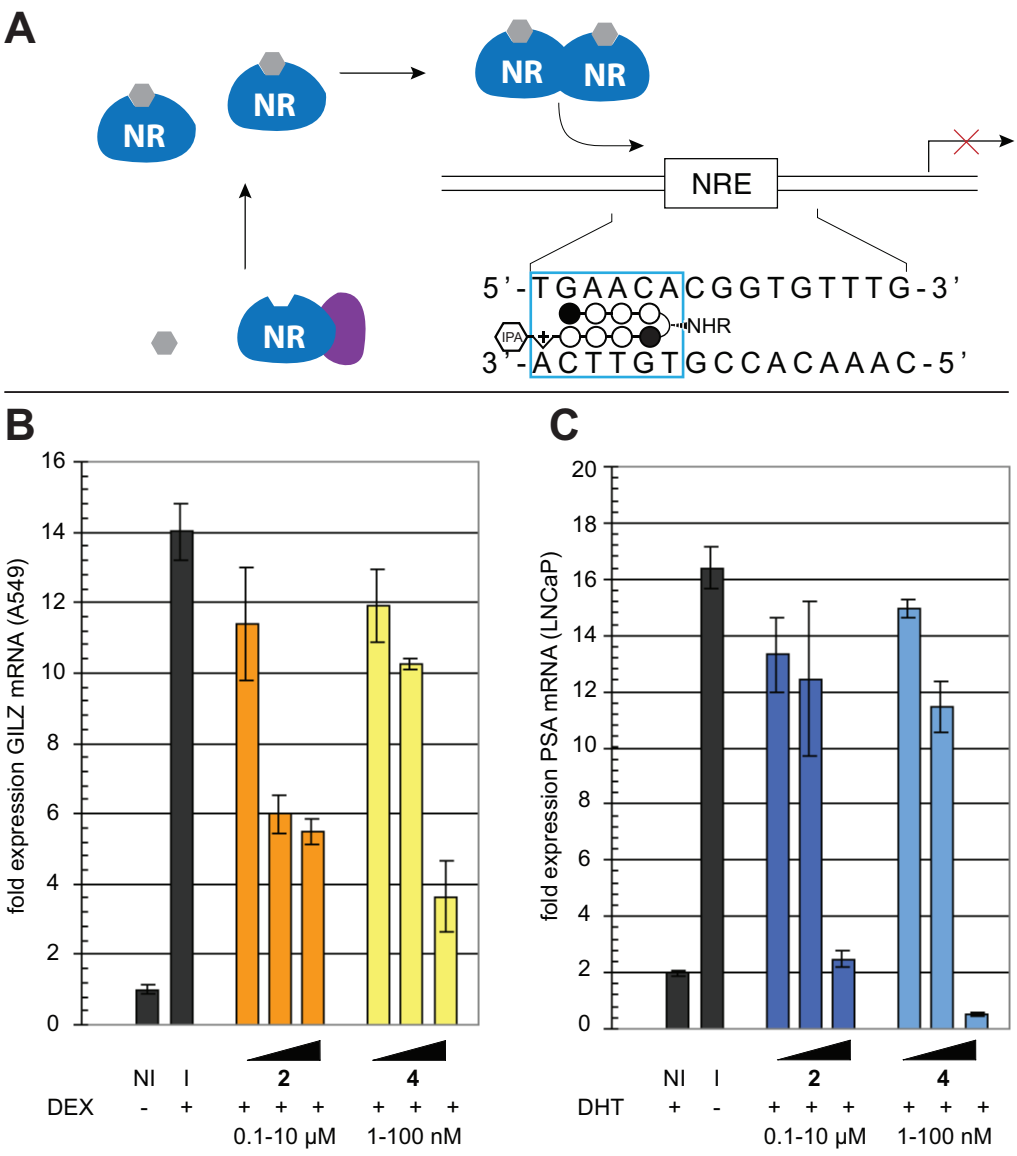

Figure 2.4: Inhibition of nuclear-receptor mediated gene expression by β-aryl polyamides. (a) General schematic of nuclear receptor-mediated gene expression and polyamide inhibition of the protein-DNA interface. (b) Effect of β-turn polyamides **2** and **4** on dexamethasone (DEX)-induced *GILZ* gene expression as measured by qRT-PCR analysis. I = DEX-induced. NI = non-induced. Polyamide **2** concentrations: 100, 1000, 10,000 nM, polyamide **4** concentrations: 1, 10, 100 nM. (c) Effect of β-substituted polyamides **2** and **4** on dihydrotestosterone (DHT)-induced *PSA* gene expression as measured by qRT-PCR analysis. Polyamide **2** concentrations: 100, 1000, 10,000 nM, polyamide **4** concentrations: 1, 10, 100 nM. I = induced. NI = not induced.

Polyamides **1-12** target the 5'-WGWWCW-3' sequence found in the consensus glucocorticoid response element (GRE). Therefore, as an initial test of whether the

increased activity of β-aryl polyamides might be extended to gene regulatory studies, we analyzed the effects of β-aryl polyamide **4** and parent polyamide **2** on endogenous GR-mediated transcription in A549 cells. Following 48 hours treatment with **2**, **4**, or vehicle DMSO, A549 cells were induced with dexamethasone (Dex) before isolation of total RNA and analysis by qRT-PCR. As seen in Figure 2.4B, β-aryl polyamide **4** blunts GR-driven transcription of the canonical GR-regulated gene GILZ in a dose-dependent fashion.

Remarkably, inhibition of gene expression by **4** occurs at polyamide concentrations 100x lower than parent compound **2**. Similar results are seen for expression of FKBP5, another prototypical GR target (Figure 2.5).

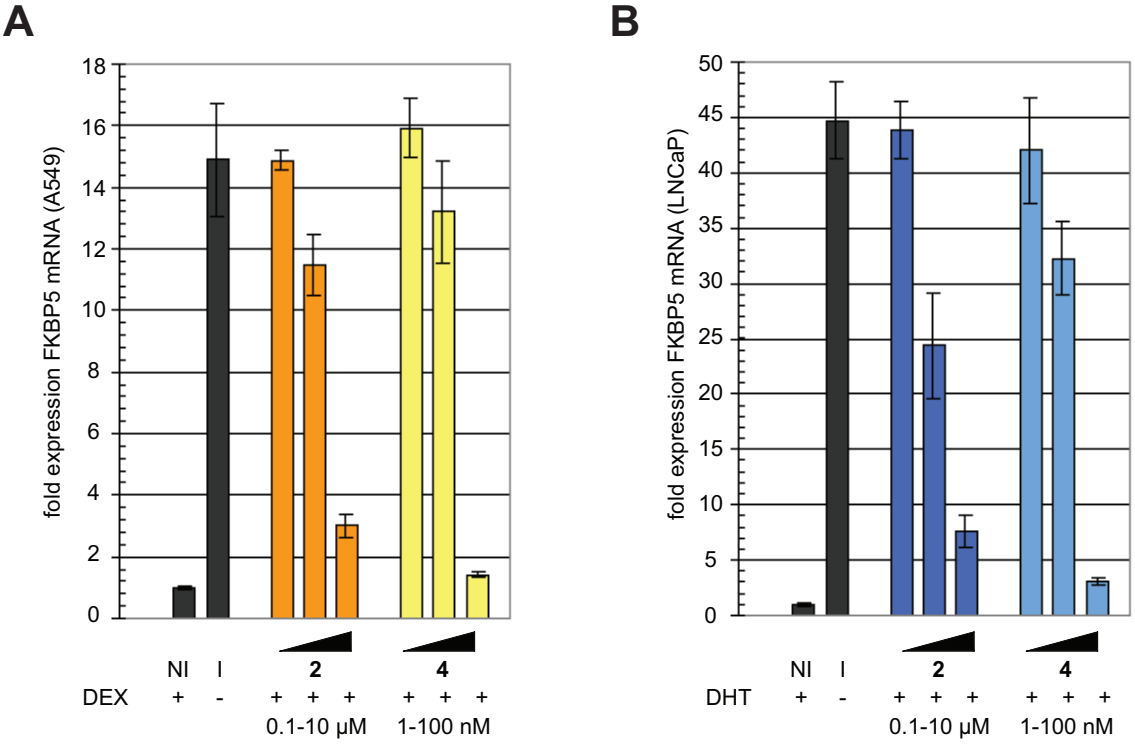

Figure 2.5: Inhibition of nuclear-receptor mediated gene expression by β-aryl polyamides. (a) Effect of β-turn polyamides **2** and **4** on dexamethasone-induced *FKBP5* gene expression as measured by qRT-PCR analysis. I = induced. NI = non-induced. Polyamide **2** concentrations: 100, 1000, 10,000 nM, polyamide **4** concentrations: 1, 10, 10 nM. (b) Effect of β-turn polyamides **2** and **4** on dihydrotestosterone-induced *FKBP5* gene expression as measured by qRT-PCR analysis. Polyamide **2** concentrations: 100, 1000, 10,000 nM, polyamide **4** concentrations: 1, 10, 10 nM. I = induced. NI = not induced.

Notably, these effects are not expected to be due to cytotoxicity, as these experiments utilize a fivefold higher cell plating density than cytotoxicity analyses and are normalized to a housekeeping gene (*GUSB*) that remains stable to polyamide treatment (Figure 2.6).

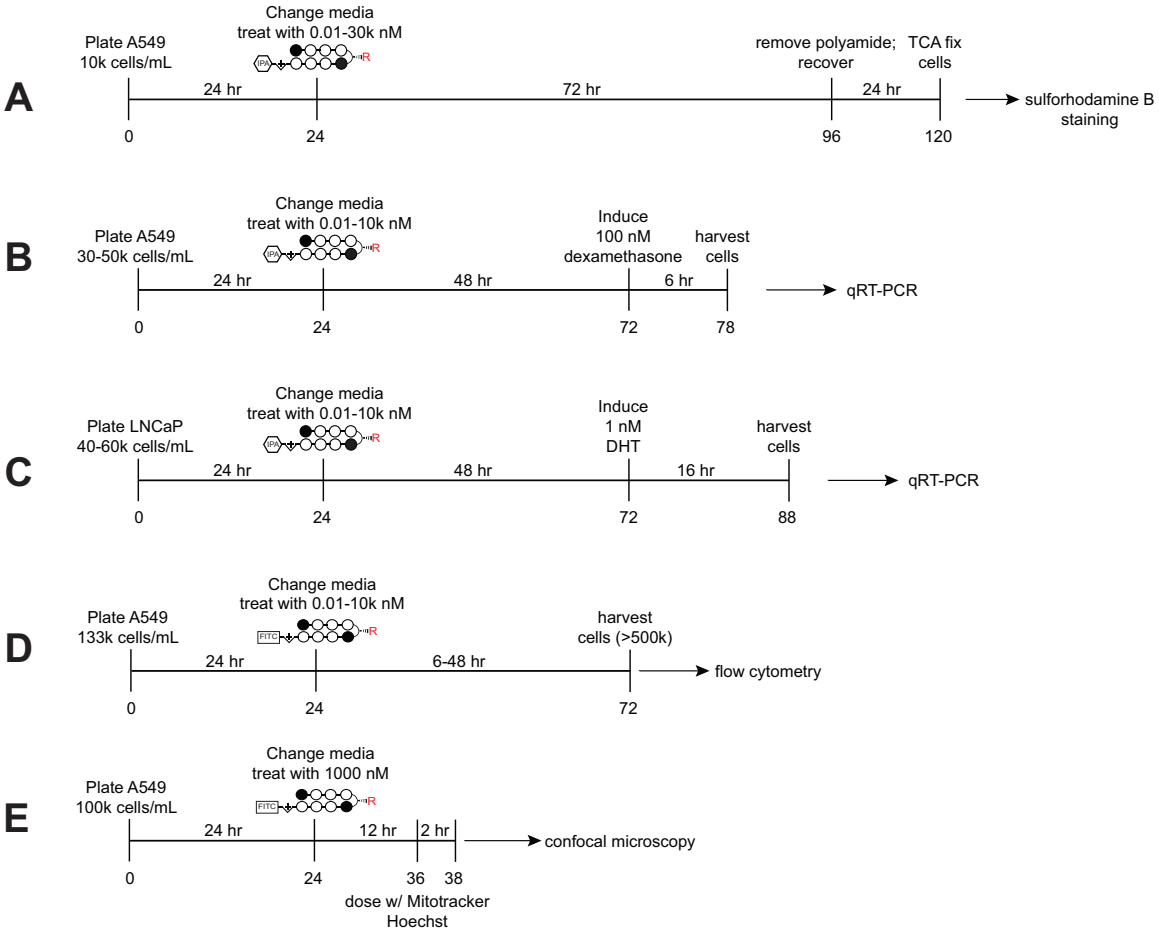

Figure 2.6: Time courses for (a) cytotoxicity analysis, (b) dexamethasone-induced gene expression studies, (c) dihydrotestosterone-induced gene expression studies, (d) flow cytometric analysis of uptake of polyamide-FITC conjugates, (e) confocal microscopy analysis of uptake of polyamide-FITC conjugates.

Time course experiments show substantial inhibition of dexamethasone-induced transcription as early as 12 hours after polyamide treatment, far prior to the onset of cytotoxicity (Figure 2.7).

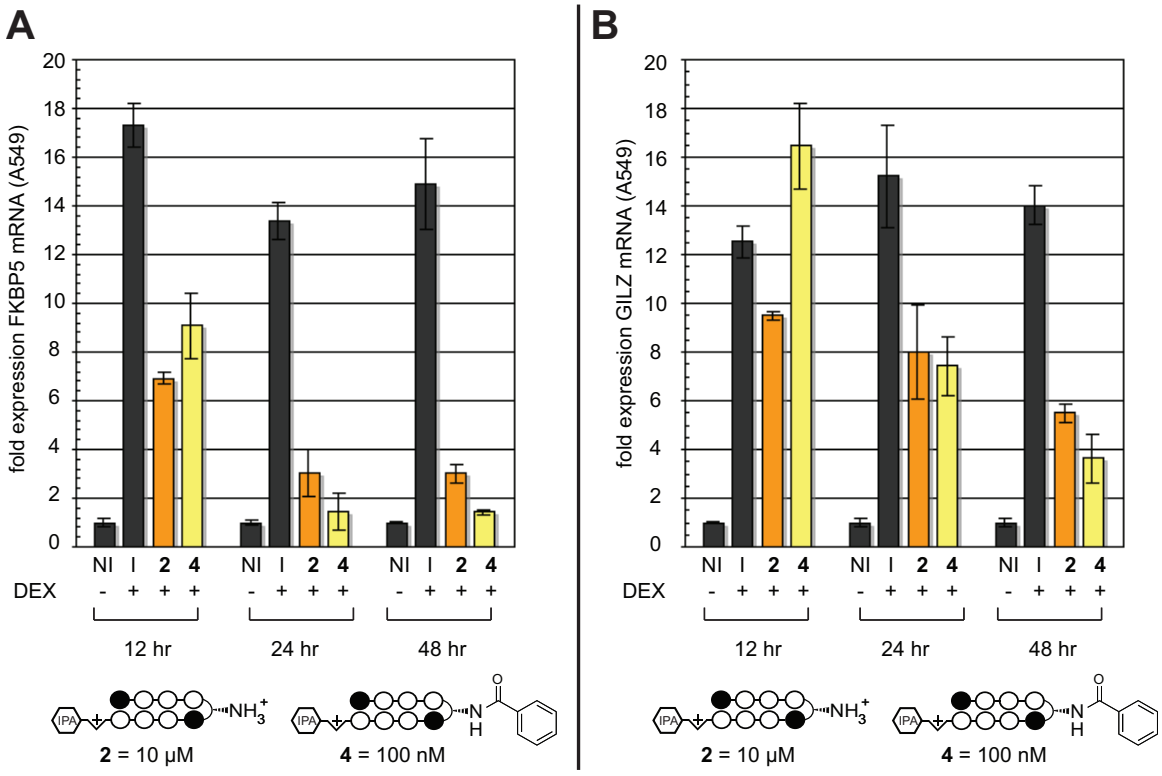

Figure 2.7: Time course analysis of polyamide-mediated inhibition of dexamethasone-induced gene expression. (a) Effect of β-turn polyamides **2** and **4** on dexamethasone (DEX)-induced *GILZ* gene expression as measured by qRT-PCR analysis. I = DEX-induced. NI = non-induced. Polyamide **2** concentration: 10,000 nM, polyamide **4** concentration: 100 nM. These concentrations of **2** and **4** were chosen because they show approximately equivalent inhibition of GR-mediate gene expression at 48 hr. (b) Identical time course analysis of polyamide inhibition of *FKBP5* gene expression over time.

Since the sequence targeted by **4**, 5'-WGWWCW-3', is also found in the androgen response element (ARE), we next tested whether **4** showed similarly enhanced inhibition of androgen receptor (AR) regulated gene expression.[7] LNCaP prostate cancer cells were exposed to polyamides **2** or **4** for 48 hours prior to induction with the AR-activating ligand 4,5α-dihydrotestosterone (DHT). Quantitative PCR analysis of reverse-transcribed mRNA shows a drastic decrease in transcription of the known AR target gene prostate specific antigen (*PSA*, also known as *KLK3*) following exposure to **4** (Figure 2.4C). Once again, this inhibition is greater than that observed when parent compound **2** is applied at 100x greater concentrations, reducing PSA mRNA to below basal (non-induced) levels. These results highlight the activity of β-aryl polyamides as potent

antagonists of nuclear receptor-mediated gene expression in living cells.

The Effect of β-Aryl Substitution on Polyamide Uptake by Quantitative Fluorescence Analysis

Hypothetically, the increased biological activity of β-aryl turn polyamides could be attributed to either 1) improved ability to impede protein-DNA interactions, 2) increased uptake, or 3) reduced efflux. The former seemed unlikely, given that our initial structure-activity analysis showed no correlation between steric bulk of the β-aryl turn, which would be expected to affect interaction of groove-binding proteins, and cytotoxicity (Figure 2.3). Therefore, to examine cellular uptake in a systematic and direct fashion we synthesized fluorescent analogues of polyamides **2** and **4** and analyzed their accumulation by confocal microscopy and flow cytometry.[11,26] Polyamide-FITC conjugates **13** and **14** show similar trends in terms of biological activity compared to parent compounds, although the observed gap in cytotoxicities is decreased from ~ 100x to ~10x (Figure 2.8).

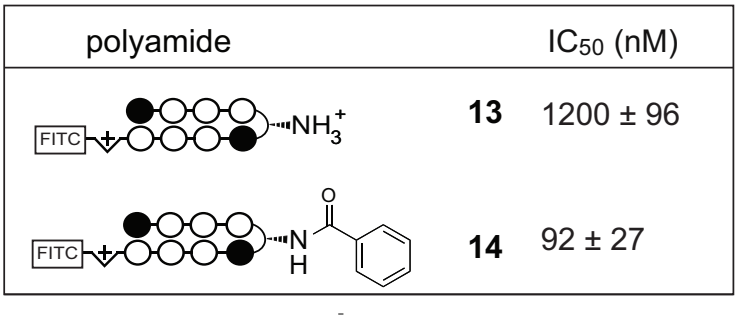

Figure 2.8: Relative cytotoxicity of fluorescent analogues **13** and **14** in A549 cells. Cytotoxicities of the parent compounds **2** and **4** are found in Figure 2.3.

Following addition to growth media, polyamides **13** and **14** penetrate the membrane and localize to the nucleus of A549 cells, as verified by co-localization with

the well-known DNA stain Hoechst (Figure 2.9A). However, flow cytometry analysis reveals quantitative differences in the kinetics and degree of uptake. Cells treated with 100 nM β-aryl polyamide **14** demonstrate a rapid increase in fluorescence intensity between 0-12 hours, compared to much slower accumulation of β-amino polyamide **13** dosed under identical conditions (Figure 2.9B).

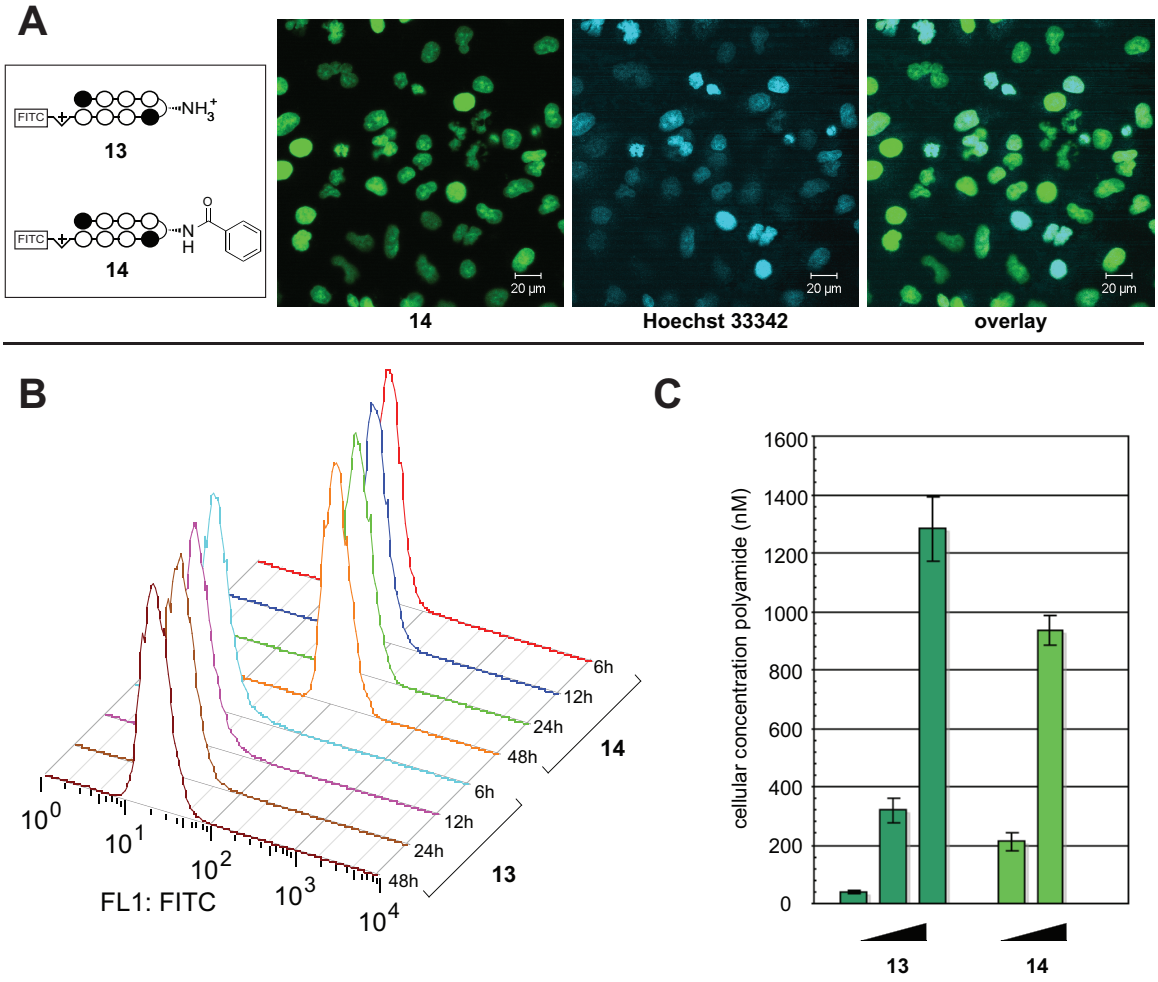

Figure 2.9: Quantitative fluorescence analysis of β-turn substitution on Py-Im polyamide nuclear uptake. (a) Nuclear localization of β-aryl polyamide **13**, as verified by co-localization with Hoechst 33342. (b) Influence of incubation time on fluorescence for A549 cells treated with 100 nM polyamide **13** or **14**. X-axis: relative median fluorescence (FL1: FITC channel); Y-axis: hours of polyamide treatment. (c) Influence of dosage concentration on nuclear accumulation of polyamides. Polyamide **13** concentration: 100 nM, 1000 nM, 10,000 nM. Polyamide **14** concentration: 100 nM, 1000 nM.

Analyzing the overall percentage of fluorescently labelled cells as compared to a DMSO-treated control shows that treatment with 100 nM **14** results in fluorescent

labelling of ~ 88% of A549 cells after 6 hr, while cells treated with 100 nM **13** show labelling of only ~5% of cells over the same time period (Figure 2.10).

A

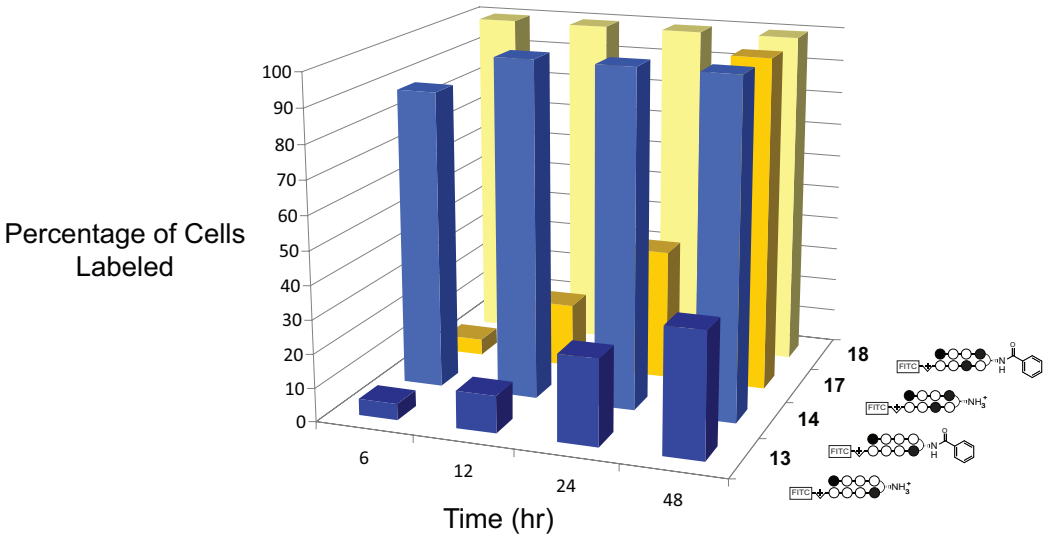

B

Polyamide	core	turn	6 hr	12 hr	24 hr	48 hr
13	GWWC	amine	4.8	11.1	25.5	36.9
14	GWWC	benzamide	88.4	99.8	99.6	99.4
15	TWCG	amine	40.0	80.3	97.8	99.5
16	TWCG	benzamide	98.8	99.7	99.6	81.3
17	GWCG	amine	4.8	19.0	38.6	98.7
18	GWCG	benzamide	99.7	99.6	99.6	99.7
19	GCGC	amine	2.1	2.9	2.0	9.1
20	GCGC	benzamide	3.8	7.3	9.2	9.8

*all compounds dosed at 100 nM

Figure 2.10: Percentage of cells labelled as a function of time exposed to β-turn polyamides β-aryl **13-20** (100 nM). (a) Bar graph depicting relative percentage of cells fluorescently labelled by β-amino polyamides **13** and **17** compared to their β-aryl analogues **14** and **18**. (b) Complete data for all polyamide cores analyzed in this study. Percentage of cells labelled is calculated relative to control cells treated with vehicle DMSO.

In order to gain a more quantitative view of the fluorescence increase, we calculated the nuclear concentrations of fluorescent polyamides **13** and **14** through comparison to fluorescent beads functionalized with known amounts of the FITC fluorophore.[14,26] Using this methodology, at 48 hours we observe a >4x greater accumulation of **14** than **13** in A549 nuclei when dosed at identical concentrations (100 nM). However, these concentrations can be shifted by increasing polyamide

concentration, as 10x greater dosage concentrations result in a ~3x increase in polyamide concentration values over 48 hours (Figure 2.9C). Notably, this is not due merely due to decreased cell growth, as analysis of cell count and viability prior to flow cytometry revealed no differences between treated samples. Finally, to differentiate uptake and efflux, we compared the effect of verapamil on uptake of β-aryl and β-amino polyamides. Verapamil is an inhibitor of the *p*-glycoprotein transporter that has previously been implicated in cellular efflux of polyamides.[27] If β-aryl polyamide **4** is attaining higher concentrations through reduced efflux, verapamil treatment should have little or no affect on intracellular polyamide concentration, whereas if β-aryl polyamide **4** is attaining higher concentrations through enhanced uptake, verapamil will have additive effect on nuclear accumulation. Our results are consistent with the latter mechanism, as we observed similarly higher fluorescent labelling by both **2** and **4** in A549 cells co-treated with a non-toxic (10 μM) dose of verapamil (Figure 2.11). Overall these findings have two implications: 1) β-aryl turns can significantly increase the rate of polyamide uptake at sub-micromolar concentrations and 2) polyamide cytotoxicity and cellular uptake are well correlated, as the 10x increase in cytotoxicity of **14** relative to **13** is mirrored by its accumulation in cells at 10x lower concentrations.

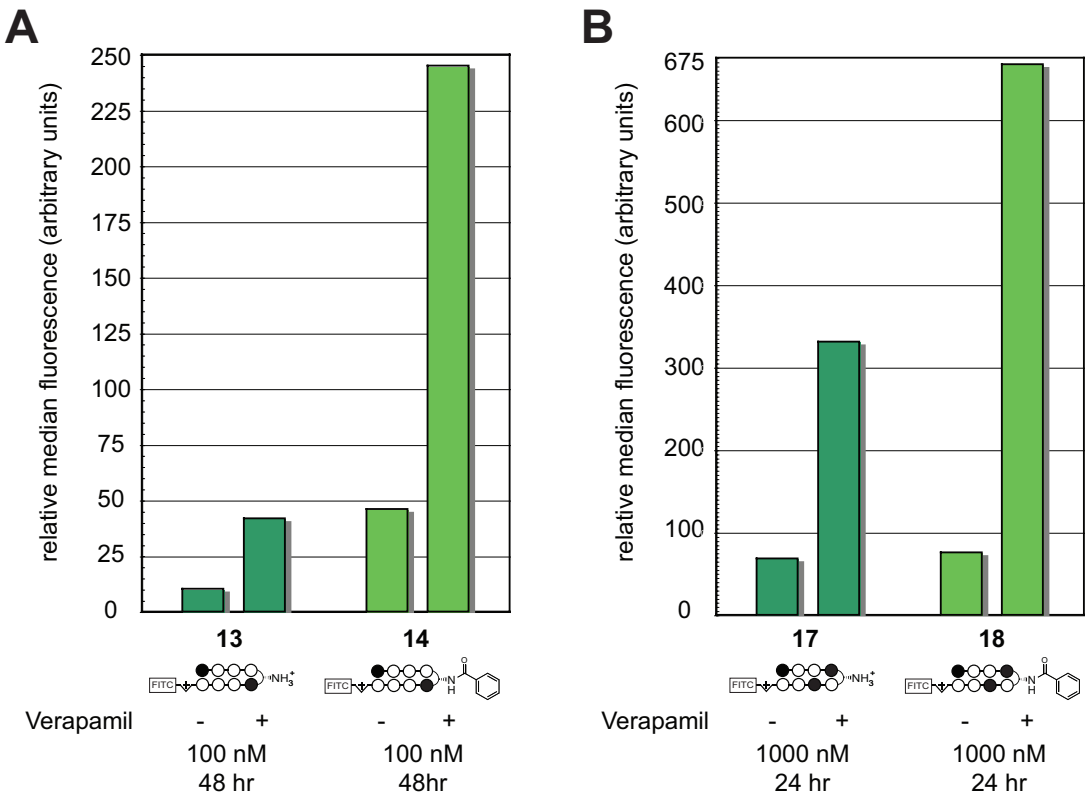

C

Polyamide	core	turn	conc. (nM)	wash (hr)	fluorescence (RMF)	%cells labeled
13	GWWC	amine	1000.0	-	125.5	99.9
			1000.0	24.0	41.4	88.4
			1000.0	48.0	32.5	79.6
14	GWWC	benzamide	100.0	-	83.5	99.8
			100.0	24.0	40.0	89.3
			100.0	48.0	36.9	67.8

*compounds incubated for 24 hr followed by removal or immediate FACS

Figure 2.11: Analysis of β-aryl (**14**) and β-amino (**13**) polyamide efflux. (a) Adherent A549 cells were incubated with 100 nM **13** or **14** in the presence or absence of verapamil (10 μM) for 48 hr and analyzed by flow cytometry. Both polyamides show similar increases in uptake. All samples were analyzed in the same biological experiment. Cellular fluorescence reported as arbitrary units. (a) Adherent A549 cells were incubated with 1000 nM **13** or **14** in the presence or absence of verapamil (10 μM) for 24 hr and analyzed by flow cytometry. Both polyamides show similar increases in uptake. (c) Washout study of polyamides. A549 cells were treated with **13** or **14** for 24 hr, at which point polyamides were removed and cells were grown in fresh media for 0, 24, or 48 hr followed by FACS analysis. Both compounds show similar profiles, suggesting efflux or dilution by cell growth proceeds similarly for each.

Exploring the Utility of β-Aryl Substitution on Alternative Polyamide Cores

Finally, we examined the ability of β-aryl turns to influence the uptake of polyamide cores targeting alternative sequence motifs. We synthesized fluorescent β-amino and β-benzamide polyamides targeting the sequences 5'-WTWCGW-3' (**15-16**),

5'-WGWCGW-3' (**17-18**), and 5'-WGCGCW-3' (**19-20**). Compound **15** is a high affinity binder of the 5'-ATACGT-3' sequence found within the hypoxia response element (HRE) of the VEGF enhancer,[6] while compounds **17**-2**0** probe the ability of β-aryl turns to facilitate the uptake of polyamides with increased N-methylimidazole content, a known negative determinant of polyamide nuclear localization.[12,14] Next, uptake was verified by confocal microscopy (Figure 2.12).

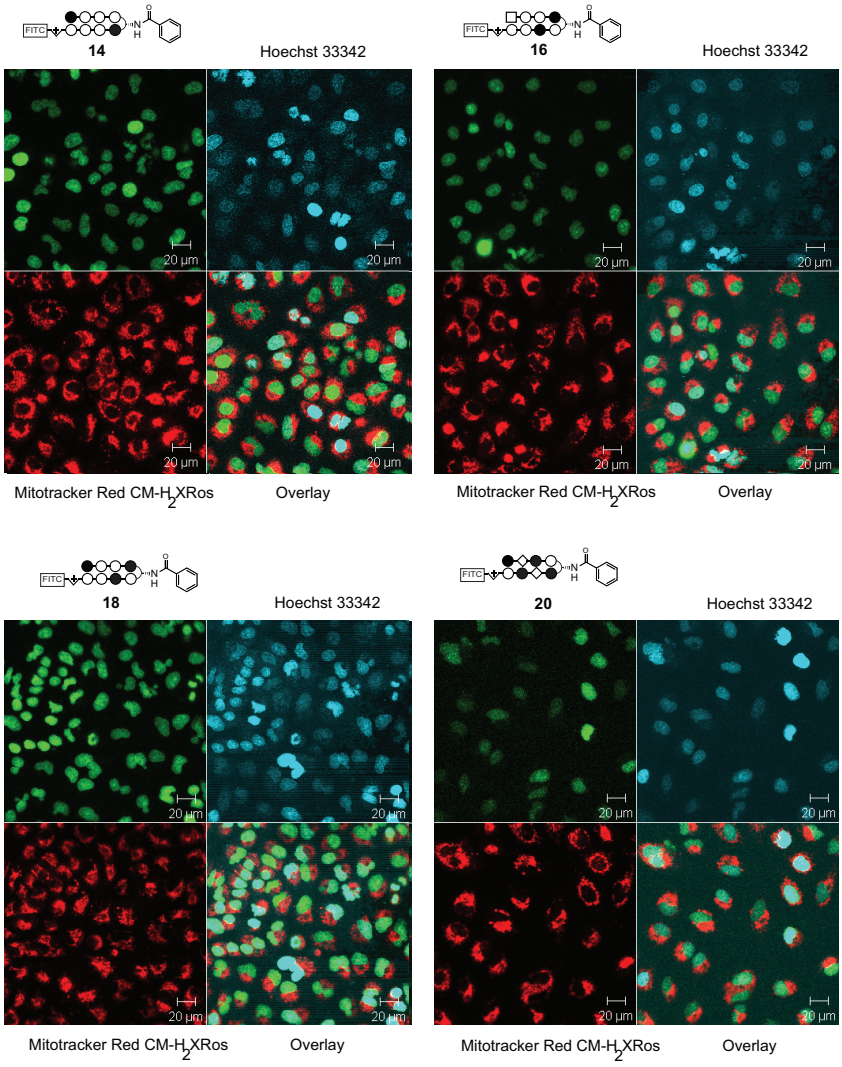

Figure 2.12: Confocal microscopy analysis of β-aryl polyamide nuclear localization. Adherent A549 cells were treated with 1μM β-aryl polyamide-FITC conjugates (**14**/**16**/**18**/**20**) for 16 hr, and counterstained with Hoechst 33342 (nuclear stain) and Mitotracker Red CM-H_2Ros (mitochondrial stain) just prior to imaging. Top left: polyamide-FITC (λ_{ex} = 488 nm λ_{em} = 505-530 nm). Top right: Hoechst (λ_{ex} = 750 nm [2-photon] λ_{em} = 390-465 nm). Bottom left: Mitotracker (λ_{ex} = 543 nm λ_{em} = 565-615 nm). Bottom right: three-color overlay.

Each compound was further analyzed for time and concentration-dependent uptake by quantitative flow cytometry (Figures 2.13 and 2.14). When added to media at 100 nM, time-course experiments demonstrate that polyamide-FITC conjugates **15**-**18** rapidly accumulate in A549 cells (Figure 2.13). Analysis of Im-rich polyamide **19**-**20** at 100 nM was less informative, as these compounds required dosing at 1000 nM to label a significant percentage of treated cells (Figure 2.10).

A

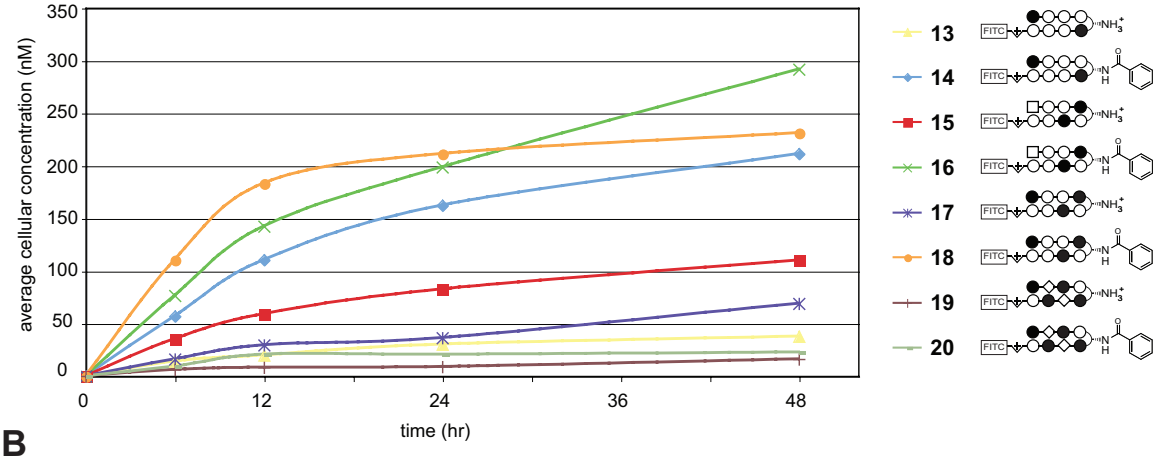

B

Polyamide	core	turn	6 hr	12 hr	24 hr	48 hr
13	GWWC	amine	13.9 (± 0.9)	20.1 (± 0.2)	30.3 (± 1.8)	37.6 (± 5.1)
14	GWWC	benzamide	57 (± 3.4)	110.6 (± 5.0)	162.4 (± 15.0)	211.3 (± 31.4)
15	TWCG	amine	35.4 (± 0.4)	59.2 (± 7.1)	82.6 (± 7.5)	110.2 (± 19.5)
16	TWCG	benzamide	76.4 (± 6.0)	142.6 (± 7.7)	198.6 (± 4.4)	291.5 (± 17.6)
17	GWCG	amine	16.3 (± 1.3)	29.4 (± 4.2)	36.5 (± 2.0)	69.0 (± 7.6)
18	GWCG	benzamide	110.6 (± 1.1)	183.4 (± 12.4)	211.5 (± 4.8)	231.4 (± 12.1)
19	GCGC	amine	6.1 (± 1.1)	8.1 (± 1.5)	8.8 (± 1.4)	16.1 (± 5.3)
20	GCGC	benzamide	9.3 (± 0.1)	20.5 (± 1.1)	20.7 (± 3.1)	22.8 (± 0.7)

*all compounds dosed at 100 nM; calculated cellular concentrations reported in nM

Figure 2.13: Time course analysis of uptake of polyamide-FITC conjugates incorporating diverse DNA sequence-recognition elements. (a) Cellular concentration of polyamide-FITC conjugates **13**-**20** as a function of time incubated with A549 cells. Polyamide structures are represented as ball and stick models according the shorthand code: closed circle, Im monomer; open circle, Py monomer; diamond, β-alanine; square, 3-chlorothiophene 2-carboxylic acid. Complete structures can be found in Supplementary Data. Cellular concentration calculated from flow cytometry data as described in materials and methods. (b) Data displayed in tabular form with standard deviations. Core = DNA sequence targeted by the hairpin polyamide core heterocylic ring pairs. Turn = identity of β-turn modification.

Under these treatment conditions (100 nM **15-18**; 1000 nM **19-20**) each β-aryl polyamide shows increased cellular uptake relative to its β-amino counterpart, demonstrating the general utility of this modification in promoting increased uptake (Figure 2.14).

A

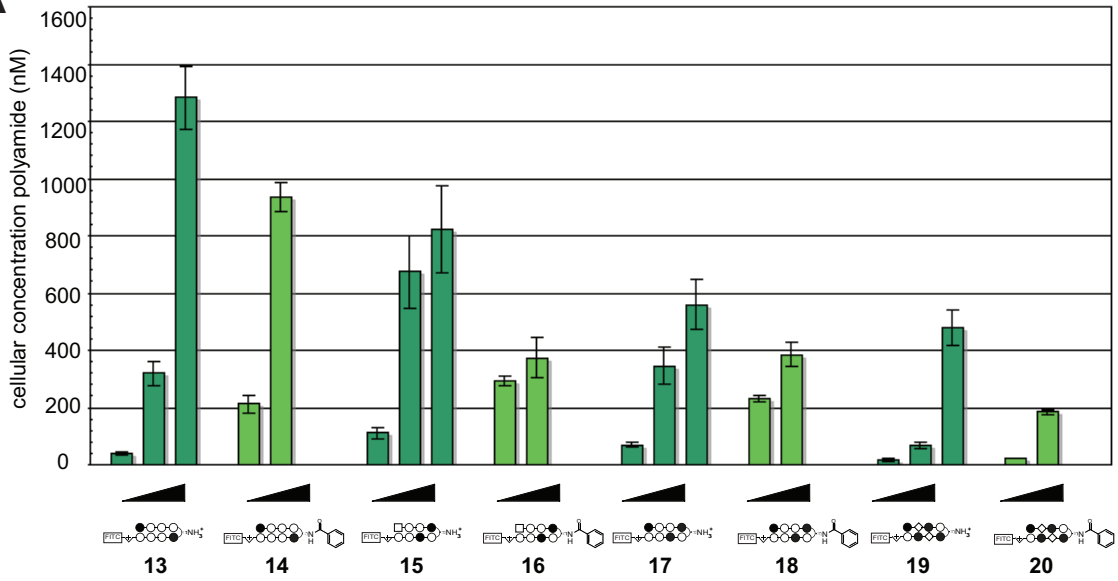

B

Polyamide	core	turn	100 nM	1000 nM	10,000 nM
13	GWWC	amine	37.6 (± 5.1)	318.5 (± 44.3)	1282 (± 107.7)
14	GWWC	benzamide	211.3 (± 31.4)	936.5 (± 51.3)	-
15	TWCG	amine	110.2 (± 19.5)	674.4 (± 126.7)	820.8 (± 151.7)
16	TWCG	benzamide	291.5 (± 17.6)	374.4 (± 71.1)	-
17	GWCG	amine	69.0 (± 7.6)	344.9 (± 65.6)	558.5 (± 87.9)
18	GWCG	benzamide	231.4 (± 12.1)	385 (± 40.4)	-
19	GCGC	amine	16.1 (± 5.3)	68.5 (± 10.4)	480.2 (± 61.3)
20	GCGC	benzamide	22.8 (± 0.7)	183.4 (± 7.9)	-

*compounds incubated for 48 hr at concentration listed in column heading; calculated cellular concentrations reported in nM

Figure 2.14: Influence of polyamide dosage on cellular concentration at 48 hr. (a) Graphical depiction of relative cellular concentrations of polyamides analyzed in this study. β-amino polyamides 13, 15, 17, and 19 were dosed at 100, 1000, and 10,000 nM respectively (left to right). β-aryl polyamides 14, 16, 18, and 20 were dosed at 100 and 1000 nM respectively (left to right). Attempts to dose β-aryl compounds at higher concentrations were hindered by insolubility. Cellular concentration calculated from flow cytometry data as described in materials and methods. (b) Data displayed in tabular form with standard deviations. Core = DNA sequence targeted by the hairpin polyamide core heterocylic ring pairs. Turn = identity of β-turn modification.

This enhanced uptake is accompanied by a large increase in the cytotoxicity of non-fluorescent analogues of Im-rich polyamides **18** and **20**, but surprisingly not 5'-WTWCGW-3' targeting polyamide **16** (Figure 2.15).

polyamide	R:		IC_{50} (nM)
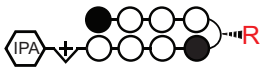	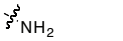	**2**	3200 ± 900
	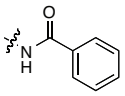	**4**	35 ± 9
	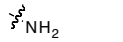	**21**	5200 ± 800
	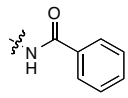	**22**	>1000
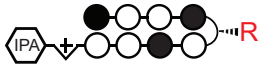	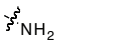	**23**	>30,000
	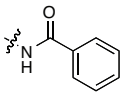	**24**	580 ± 33
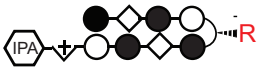	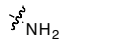	**25**	10000 ± 280
	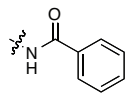	**26**	530 ± 26

Figure 2.15. Cytotoxicity of β-aryl polyamide cores conjugated to C-terminal isophthalic acid (IPA) tails in A549 cells. Complete structures are given in Scheme S2.4.

Once again flow cytometric analysis proved informative in explaining this unexpected observation, as A549 cells dosed at increasing concentrations (100 nM–10 μM) of **15-16** show concentration-dependent accumulation of parent polyamide **15**, while β-aryl polyamide **16** shows relatively equivalent uptake at both 100 nM and 1000 nM (Figure 2.14). This is consistent with the small, but constant, inhibitory effect polyamide **15** has on HIF1-α-mediated transcription, as judged by qRT-PCR analysis of VEGF gene expression (Figure 2.16).

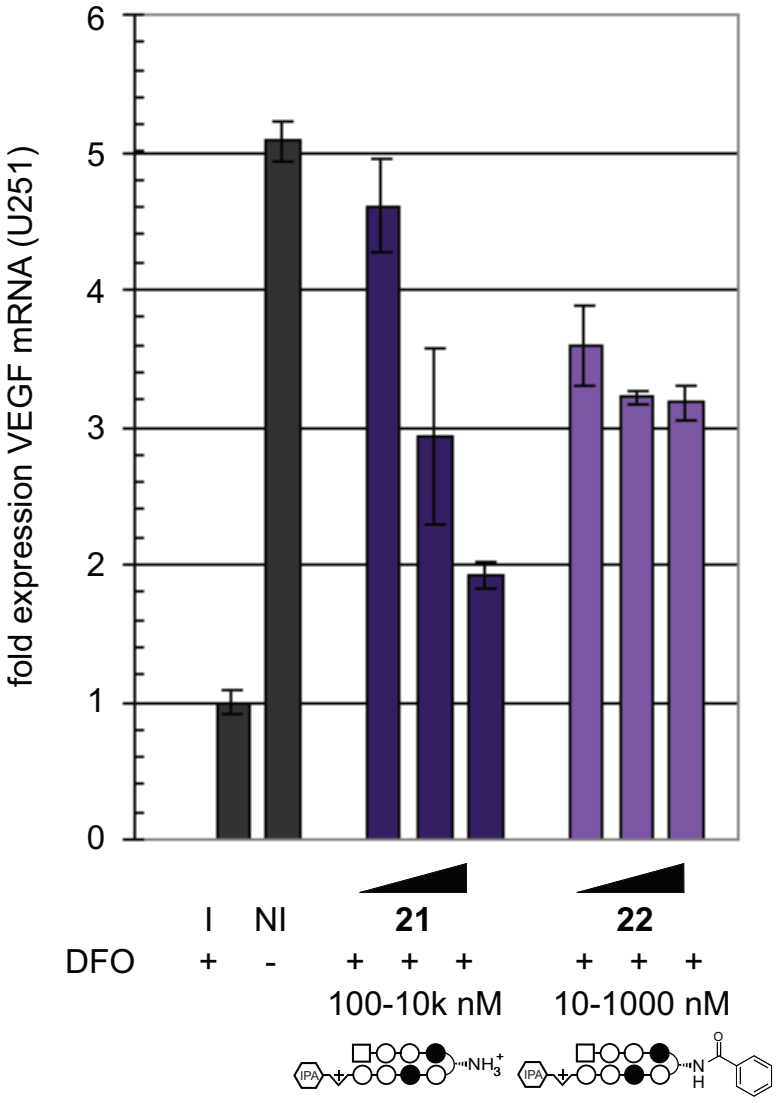

Figure 2.16. Inhibition of hypoxia-induced gene expression by β-turn polyamides targeted to the hypoxia response element (HRE) of the vascular endothelial growth factor (*VEGF)* locus. The effect of β-substituted polyamides **21** and **22** on desferoxamine (DFO)-induced *VEGF* gene expression was analyzed by qRT-PCR analysis. I = DFO induced. NI = non-induced. Polyamide **21** concentrations: 100, 1000, 10,000 nM. Polyamide **22** concentrations: 10, 100, 1000 nM.

Therefore, while our studies show β-aryl turns provide a generally applicable approach to increase the uptake of polyamides at reduced concentrations, this modification can have a variable consequence on the upper limits of polyamide nuclear accumulation that may be required for biological effects.

Conclusions

Chemical approaches for controlling gene expression at the protein-DNA interface require efficient nuclear delivery of gene regulatory agents. Thus far, comprehensive efforts to define structure-uptake relationships for hairpin polyamides in cell culture have largely focused on the optimization of the C-terminus. Insights from these studies are reflected in our use of polyamides modified with a C-terminal isophthalic acid modification for gene regulation and cytotoxicity studies (**1-12**, **21-26**), with the higher molecular weight FITC reserved for direct analysis of polyamide uptake (**14-20**).[12,15] Here we explore integration of an additional uptake determinant at the hairpin polyamide β-aminobutyric acid turn. Introduction of functionality at the polyamide turn position has previously been most thoroughly explored in the design of covalent sequence-selective DNA alkylating agents.[28,29] Our findings here represent an initial inquiry into the effect of turn modification on noncovalent sequence-selective DNA-binding agents, and have lead to the discovery of a polyamide (**4**) that exhibits excellent affinity for DNA and nanomolar inhibition of dexamethasone and DHT-induced gene expression in human cancer cells. This molecule represents one of the most biologically potent members of this compound-class (eight-ring hairpin polyamides) identified to date.

The second phase of this study examined the mechanism and generality of β-aryl turn modification as a vehicle for increasing polyamide potency using fluorescent polyamide conjugates and quantitative flow cytometry analysis. The power of this approach lies in its relatively simple calibration and ability to sample a large number of cells for any given condition. Our findings indicate the β-aryl turn of **14** aids polyamide

uptake, allowing rapid permeation and nuclear accumulation as compared to β-amino-modified **13**. When extended to hairpin polyamides with alternative heterocycle composition and DNA-binding preferences (**15-20**), uptake of polyamide-FITC conjugates was well-correlated with cytotoxicity and gene regulatory effects, implicating membrane permeability as a primary determinant of the biological activity for this class of molecules. However, while informative, these methods are not without caveats. First, the calculated nuclear concentrations cannot be taken as absolute values, as they do not take into account the known fluorescence enhancements exhibited by polyamide-FITC conjugates upon binding to DNA,[30] subcellular localization, fluorescein photostabilty, or differences in the optical properties of cells as compared to fluorochrome-coated beads. Second, fluorescein modification can significantly alter the biological properties of hairpin polyamides (compare the IC_{50} of **4** with **14**; Figure 2.8). Integration of a low molecular weight reporter into the hairpin polyamide scaffold is therefore attractive from the standpoint of streamlining activity and uptake assays. This approach may benefit from recent incorporation of click chemistry methods into many flow cytometry workflows.[31,32]

It is interesting to speculate as to the mechanism by which β-aryl turns expedite polyamide uptake. Studies of oligonucleotide-based therapies have shown that modification of these agents with highly lipophilic moieties, such as cholesterol, can facilitate association with the cell membrane and endocytosis.[33,34] It is possible a similar effect mediates the delivery of β-aryl polyamides. Also interesting is the lack of nuclear accumulation of β-aryl polyamide **16** at higher concentrations. The finding that β-aryl modification promotes increased uptake at 100 nM but not 1000 nM suggests this may

result from a physical phenomena such as insolubility (due to aggregation) at the higher concentration. In general, β-aryl polyamides show decreased solubility relative to β-amino compounds owing to their reduced charge at physiological pH.

Other than delivery, perhaps the most important future challenge lies in developing new methods to define the concentration-dependent effects of Py-Im polyamides on gene expression in living cells. Analytical techniques such as MPE footprinting and affinity cleavage have proven essential to the design of sequence-selective DNA-binding agents,[35,36] and reveal dose-dependent binding patterns that can be used to directly guide applications *in vitro*.[37,38] Quantitative fluorescence analysis of polyamide uptake, as performed here, combined with recently developed high-throughput sequencing strategies for analysis of protein-DNA binding[39,40] and gene expression[39] represent promising approaches to similarly footprint polyamide-induced perturbations and binding events *in vivo*, and thereby define the relationship between nuclear concentration and gene regulatory effects.

Overall, these findings highlight hairpin turn modification as a promising new strategy for intracellular delivery of Py-Im polyamides. In terms of applications, the increased potency of these analogues should prove immediately useful for testing in animal models, where the ability to work at lower concentrations will help overcome technical challenges of polyamide solubility and formulation. The amenability of the β-aryl turn to substitution also raises the possibility of using it as a selective handle to optimize polyamide pharmacokinetic properties, such as plasma protein binding, through attachment of pendant chemical functionalities. Finally, β-aryl turns may prove useful for the delivery of molecular probes using polyamides as tethered DNA-binding domains

into living cells. The relevance of such strategies is highlighted by the numerous studies which have used polyamides to target the activity of alkylating agents,[28] chromatin remodelling enzymes,[41] and transcriptional activation domains[42-43] to subsets of genomic loci. Future work will focus on characterizing the mechanism of β-aryl polyamide uptake and applying this technology to the manipulation of protein-DNA interactions in living systems.

Materials and Methods

Reagents and Equipment

Anhydrous N,N-dimethylformamide (DMF), diisopropylethylamine (DIEA), triethylsilane (Et3SiH), trifluoroacetic acid (CF3CO2H [peptide synthesis grade]), isophthalic acid, and (±)-verapamil hydrochloride were purchased from Sigma-Aldrich. Fluorescein isothiocyanate (FITC, Isomer I) was purchased from Invitrogen. Kaiser oxime resin (LL, 200-400 mesh) and benzotriazole-1-yl-oxy-trispyrrolidinophosphonium hexafluorophosphate (PyBOP) were from Novabiochem. N-β-Cbz-N-γ-Boc-D-3,4-diaminobutyric acid [Z-D-β-Dab(Boc)-OH] was purchased from Sigma Aldrich (product code 28206). All Boc-protected *N*-methylpyrrole and *N*-methylimidazole monomers and dimers for polyamide synthesis were prepared according to the published protocols.[44-45] Bulk grade solvents were purchased from Fisher Scientific. Centrifugation was performed in a Beckman Coulter bench-top centrifuge (Allegra 21R) equipped with a Beckman swing-out rotor (model S4180). Preparative HPLC purification was performed on an Agilent 1200 Series instrument equipped with a Phenomenex Gemini preparative column (250 x 21.2 mm, 5μm) with the mobile phase consisting of a gradient of acetonitrile (MeCN) in 0.1% CF3CO2H (aqueous). Polyamide synthesis was monitored by analytical HPLC, with analysis conducted on a Beckman Gold instrument equipped with a Phenomenex Gemini analytical column (250 x 4.6 mm, 5μm), a diode array detector, and the mobile phase consisting of a gradient of MeCN in 0.1% CF3CO2H (aqueous). Polyamide concentrations were measured by UV analysis on a Hewlett-Packard model 8453 diode array spectrophotometer in distilled and deionized water (ddH2O) with a molar extinction coefficient (ε) of 69,500 $M^{-1}cm^{-1}$ at λ_{max} of 310 nm.

Synthesis of Polyamides

All polyamide cores were synthesized by manual solid-phase synthesis on Kaiser oxime resin (Novabiochem) according to the previously published protocol.[19] Polyamides were cleaved from resin by aminolysis with 3,3'-diamino-N-methyldipropylamine for 3 hr at 55°C. Repeated cycles of precipitation and washing with diethyl ether were used to remove excess 3,3'-diamino-N-methyldipropylamine from polyamides prior to purification by reverse phase HPLC.[20] The purified polyamide cores were modified at the C-terminal tail position by isophthalic acid (IPA) or fluorescein-5-isothiocyanate (FITC isomer I; Invitrogen) as previously described.[15] Polyamides incorporating the β-Cbz-γ-aminobutyric acid turns were subjected to repeated cycles of precipitation and washing with diethyl ether to remove excess reagents, resuspended in 9:1 CF_3COOH/TFMSA (0.9 mL, 5 min) to remove the benzyl carbamate group,[21] and purified by HPLC to afford polyamides bearing a β-amino group at the turn. These compounds were coupled to the designated acids by PyBOP and subjected to a final step of HPLC purification to yield β-aryl turn conjugates. Purity of all compounds was verified by analytical HPLC and matrix-assisted, LASER desorption/ionization time-of-flight (MALDI-TOF) mass spectrometry.

General Synthetic Procedure for Conjugation of β-Aryl Turn

A solution of benzoic acid (2.4 mg, 0.02 mmol) and PyBOP (10.4 mg, 0.02 mmol) in DIEA (14 μL, 0.2 mmol) and DMF (0.4 mL) was stirred at 23°C for 1 hr. Separately, polyamide **2** (800 nmol) was dissolved in DMF (0.1 mL) and slowly added to the pre-activated isophthalic acid solution. The reaction was allowed to stand at 23°C for 1 hr and

monitored by analytical HPLC. Upon completion, Et_2O (45 mL) was added and the reaction was vortexed thoroughly, resulting in formation of a brownish white precipitate that was isolated by centrifugation (~ 4500 rpm).[46] After removal of the organic layer, the residual solid was dissolved in DMF (0.5 mL) with ultrasonication, and diluted with 20% MeCN in 0.1% CF_3COOH (4.5 mL). Purification by reverse-phase HPLC followed by lyophilization provided β-aryl polyamide **4** (0.082 mmol, 91%). MS (MALDI-TOF) calc'd for $C_{72}H_{81}N_{22}O_{13}$ $[M+H]^+$ 1461.6, found 1461.9.

Polyamide Characterization Data

1 MS (MALDI-TOF) calc'd for $C_{65}H_{76}N_{21}O_{12}$ $[M+H]^+$ 1342.6, found 1589.8.
2 MS (MALDI-TOF) calc'd for $C_{65}H_{77}N_{22}O_{12}$ $[M+H]^+$ 1357.6, found 1357.8.
3 MS (MALDI-TOF) calc'd for $C_{67}H_{79}N_{22}O_{13}$ $[M+H]^+$ 1399.6, found 1399.9.
4 MS (MALDI-TOF) calc'd for $C_{72}H_{81}N_{22}O_{12}$ $[M+H]^+$ 1461.6, found 1461.9.
5 MS (MALDI-TOF) calc'd for $C_{71}H_{80}N_{23}O_{13}$ $[M+H]^+$ 1462.6, found 1462.7.
6 MS (MALDI-TOF) calc'd for $C_{72}H_{80}N_{23}O_{15}$ $[M+H]^+$ 1506.6, found 1506.5.
7 MS (MALDI-TOF) calc'd for $C_{72}H_{82}N_{23}O_{13}$ $[M+H]^+$ 1476.6, found 1476.2.
8 MS (MALDI-TOF) calc'd for $C_{78}H_{85}N_{22}O_{13}$ $[M+H]^+$ 1537.7, found 1537.5.
9 MS (MALDI-TOF) calc'd for $C_{73}H_{81}N_{22}O_{15}$ $[M+H]^+$ 1505.6, found 1505.8.
10 MS (MALDI-TOF) calc'd for $C_{73}H_{81}N_{22}O_{15}$ $[M+H]^+$ 1505.6, found 1505.8.
11 MS (MALDI-TOF) calc'd for $C_{78}H_{93}N_{24}O_{14}$ $[M+H]^+$ 1589.7, found 1589.8.
12 MS (MALDI-TOF) calc'd for $C_{78}H_{93}N_{24}O_{14}$ $[M+H]^+$ 1589.7, found 1589.8.
13 MS (MALDI-TOF) calc'd for $C_{78}H_{83}N_{23}O_{14}S$ $[M+H]^+$ 1597.6, found 1598.0.
14 MS (MALDI-TOF) calc'd for $C_{85}H_{87}N_{23}O_{15}S$ $[M+H]^+$ 1701.6, found 1701.8.
15 MS (MALDI-TOF) calc'd for $C_{77}H_{80}N_{22}O_{14}S_2Cl_1$ $[M+H]^+$ 1635.5, found 1635.6.
16 MS (MALDI-TOF) calc'd for $C_{84}H_{83}N_{22}O_{15}S_2Cl_1$ $[M+H]^+$ 1738.6, found 1738.3.
17 MS (MALDI-TOF) calc'd for $C_{77}H_{80}N_{24}O_{14}S_1$ $[M+H]^+$ 1596.6, found 1596.8.
18 MS (MALDI-TOF) calc'd for $C_{84}H_{86}N_{24}O_{15}S_1$ $[M+H]^+$ 1702.6, found 1702.8.
19 MS (MALDI-TOF) calc'd for $C_{70}H_{80}N_{23}O_{14}S_1$ $[M+H]^+$ 1498.6, found 1498.9.

20 MS (MALDI-TOF) calc'd for $C_{77}H_{83}N_{23}O_{15}S_1$ $[M+H]^+$ 1601.6, found 1601.7.

21 MS (MALDI-TOF) calc'd for $C_{64}H_{73}N_{21}O_{12}S_1Cl_1$ $[M+H]^+$ 1394.5, found 1394.6.

22 MS (MALDI-TOF) calc'd for $C_{71}H_{76}N_{21}O_{13}S_1Cl_1$ $[M+H]^+$ 1497.5, found 1497.7.

23 MS (MALDI-TOF) calc'd for $C_{64}H_{74}N_{23}O_{12}$ $[M+H]^+$ 1356.6, found 1356.8.

24 MS (MALDI-TOF) calc'd for $C_{71}H_{77}N_{23}O_{13}$ $[M+H]^+$ 1459.6, found 1459.6.

25 MS (MALDI-TOF) calc'd for $C_{57}H_{73}N_{22}O_{12}$ $[M+H]^+$ 1257.6, found 1257.5.

26 MS (MALDI-TOF) calc'd for $C_{64}H_{76}N_{22}O_{13}$ $[M+H]^+$ 1360.6, found 1360.8.

Synthetic Schemes

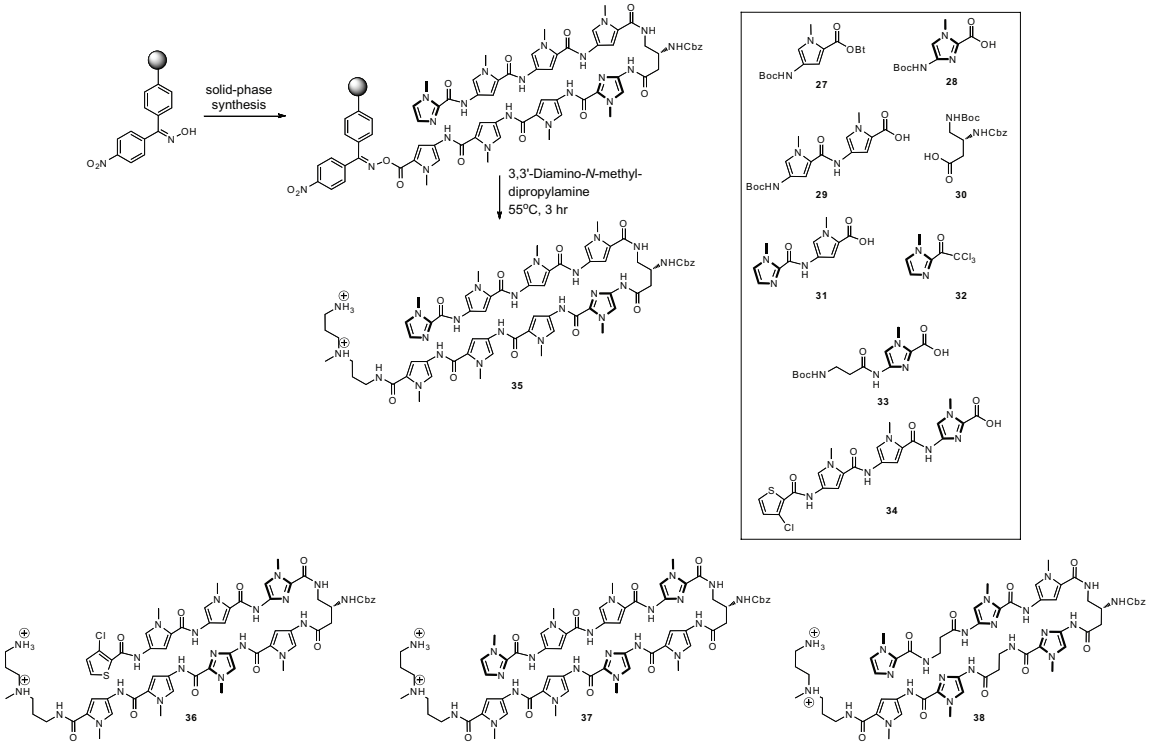

Scheme S2.1: Monomers, dimers, and general scheme for solid-phase synthesis of polyamides analyzed in this study.

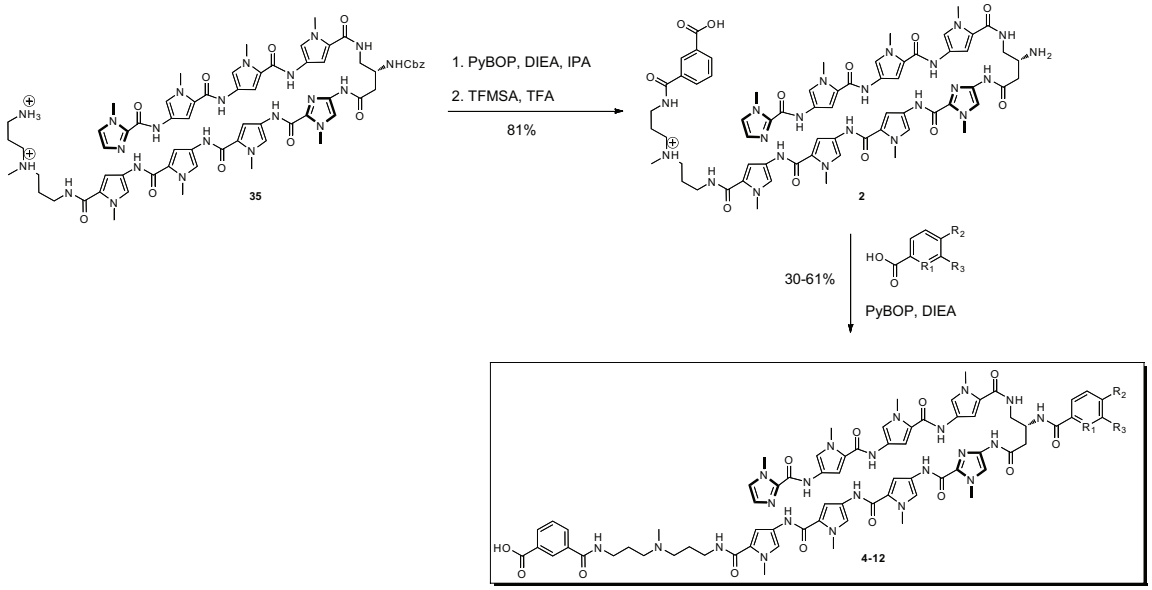

Scheme S2.2: Scheme for solution-phase derivatization of polyamides and conjugation of β-aryl turns.

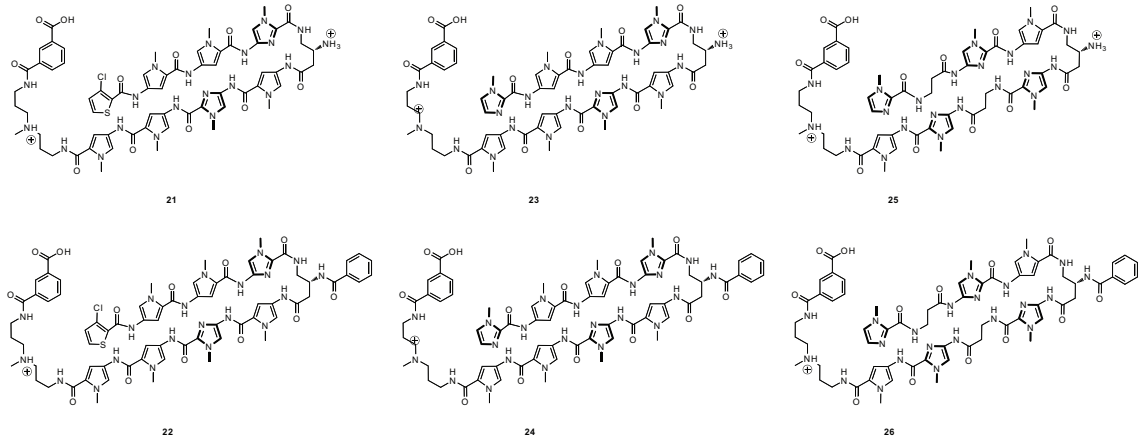

Scheme S2.3: Complete structures of polyamides **21**-**26**.

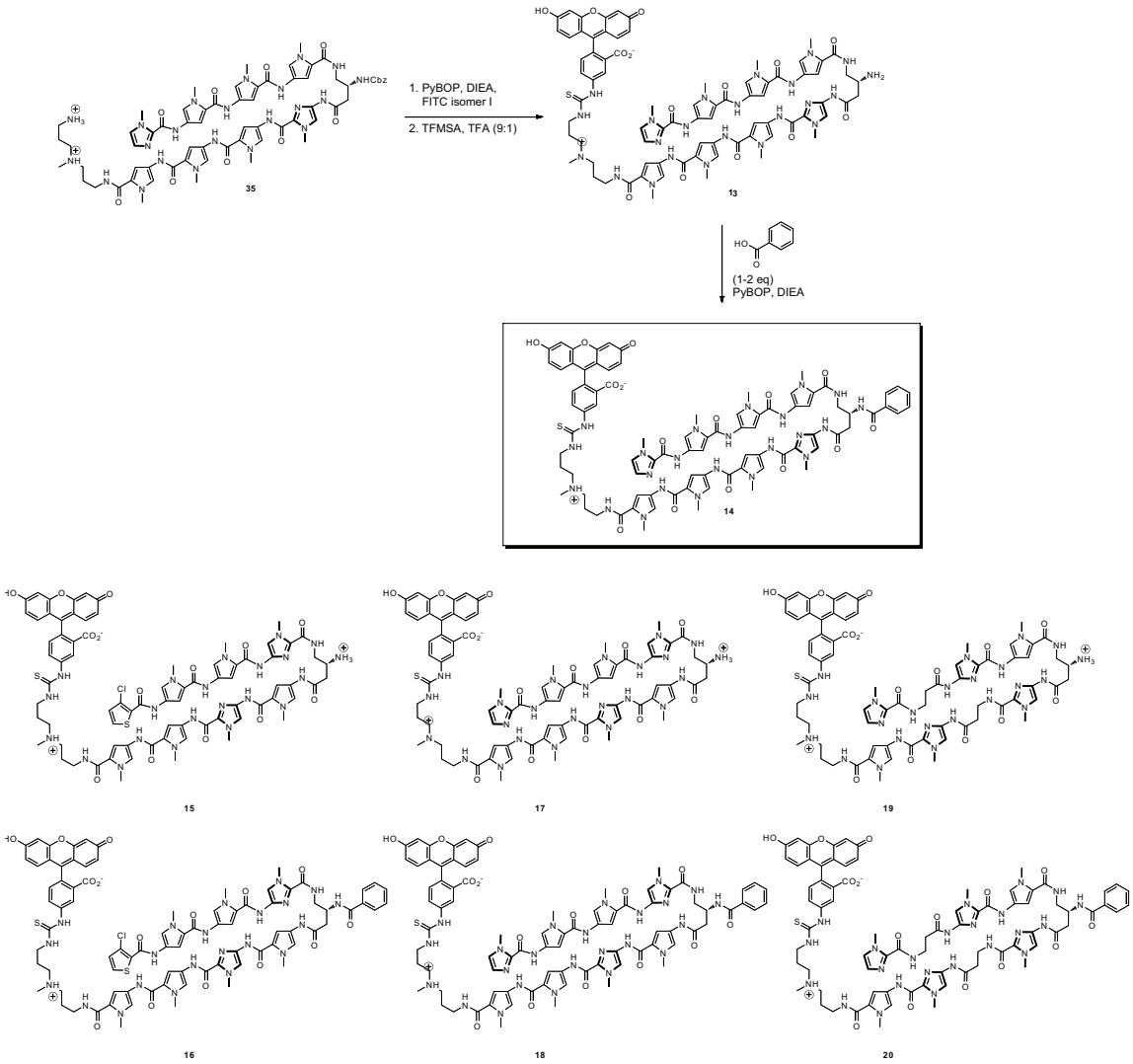

Scheme S2.4: Scheme and complete chemical structures for fluorescent polyamides **14**-**20**.

Cell Culture

All cell lines were purchased from ATCC (Manassas, VA) and maintained in the following media: A549 cells (F-12K); LNCaP (RPMI 1640); HCT-116 (McCoy's 5a Medium Modified); MCF-7 (Eagle's Minimum Essential Medium). All media were supplemented with 10% FBS and cultured at 37°C under 5% CO_2.

Sulforhodamine B Assay of Polyamide Cytotoxicity

IC_{50} values for cytotoxicity were determined in 96-well microplates using the sulforhodamine B colorimetric assay for cellular protein content as previously described.[22] All polyamide stock solutions were prepared in neat DMSO and dosed to give a final concentration of ≤ 0.3% DMSO. Briefly, cell lines were plated in 100 μL of the defined media at the following densities: A549 (1000 cells/well); LNCaP (5000 cells/well), HCT-116 (750 cells/well), MCF-7 (3000 cells/well). After 24 hr, polyamides were added to adhered cells in 100 μL of media by serial dilution. Quadruplicate wells were used for each polyamide concentration. After 72 hr, the medium was replaced with 100 μL fresh medium, and cells were allowed to recover for 24 hr. Following recovery, cells were fixed with 100 μL 10% trichloroacetic acid solution, washed, stained, and dried as described. For 48 and 72 hr polyamide treatments, the procedure was followed as above with A549 cells plated at 3000 and 2000 cells per well, respectively. After solubilization of the bound dye in 10 mM Tris (pH 8), the absorbance was measured at 490 nm on a Victor microplate reader (PerkinElmer). The data are charted as a percentage of untreated controls, corrected for background absorbance. IC_{50} is defined as the concentration that inhibits 50% of control cell growth. These values were determined

by non-linear least-squares regression fit to Y= A + (B-A)/(1+10^((Log EC50-X)*H, where A=max., B=min., and H=Hill Slope. All calculations were performed using Prism 4 (GraphPad) software. Three independent trials were averaged; stated IC_{50} values represent the mean and standard deviation.

Thermal Melting Temperature Analysis

Melting temperature analysis was performed on a Varian Cary 100 spectrophotometer equipped with a thermo-controlled cell holder possessing a cell path length of 1 cm. An aqueous solution of 10 mM sodium cacodylate, 10 mM KCl, 10 mM $MgCl_2$ and 5 mM $CaCl_2$ at pH 7.0 was used as analysis buffer. Oligonucleotides (0.1 mM stock solutions dissolved in 10 mM Tris-Cl, 0.1 mM EDTA, pH 8.0) were purchased from Integrated DNA Technologies. DNA duplexes and hairpin polyamides were mixed to a final concentration of 2 μM and 2.4 μM, respectively, for each experiment. Prior to analysis, samples were heated to 90°C and cooled to a starting temperature of 25°C with a heating rate of 5°C/min for each ramp. Denaturation profiles were recorded at λ = 260 nm from 25°C to 90°C with a heating rate of 0.5°C/min. The reported melting temperatures were defined as the maximum of the first derivative of the denaturation profile, and represent the average of four measurements.

Quantitative Real-Time Polymerase Chain Reaction (qrt-PCR) Analysis of Nuclear Receptor-Mediated Gene Expression

To analyze the effects of polyamide-treatment on dexamethasone-induced gene expression, A549 cells were plated in 24-well plates at a density of 15–25 x 10^3 cells per well (30–50 x 10^3 cells/ml).[8] After 24 hr the medium was replaced by F-12K containing 10% charcoal-stripped FBS, and polyamides were added to the specified concentrations (1-10,000 nM). Cells were incubated with polyamides for 12, 24, or 48 hr, followed by induction with dexamethasone (100 nM). After 6 hr cells were harvested and mRNA was isolated (RNEasy 96 kit - Qiagen) and reverse transcribed (Transcriptor First Strand cDNA Synthesis kit – Roche). Quantitative real-time PCR was performed with FastStart Universal SYBR Green Master Mix (Roche) on an ABI 7300 qPCR instrument (Applied Biosystems) following the manufacturer's protocol. A similar protocol was utilized to measure 4,5α-dihydrotestosterone (DHT)-induced gene expression in LNCaP cells, with the following modifications: (1) the initial plating density was 20–30 x 10^3 cells per well (40–60 x 10^3 cells/ml), (2) cells were incubated with polyamides for 48 hr, (3) cells were induced with DHT (10 nM) for 16 hr.[7] In both cases, cDNA corresponding to the genes of interest was measured relative to β-glucuronidase as an endogenous control. Primer sequences are provided in the Supplementary Data.

Confocal Microscopy Analysis

For microscopy experiments, A549 cells in F-12K medium were plated into culture dishes equipped with glass bottoms for direct imaging (MatTek) at a density of 20 x 10^3 cells per dish (100 x 10^3 cells/mL). Cells were grown in the glass-bottom dishes for 24 hr. Medium was then removed and replaced with 200 μL of fresh medium supplemented with FITC-labelled polyamides (1 μM) in DMSO (final concentration 0.1%). Cells were incubated at 37°C for 16 hr, followed by removal of media, gentle washing with 100 μL PBS, and addition of fresh medium immediately prior to imaging. For colocalization experiments, 15 μM Hoechst 33342 (0.5 mM stock in ddH_2O) and 1 μM Mitotracker Red CM-H_2XRos (1 mM stock in DMSO) were added 2 hr prior to imaging. For time-course experiments, cells were imaged directly after polyamide addition using an environmentally-controlled microscopy chamber (37 °C, 5 % CO_2). Imaging was performed at the Caltech Beckman Imaging Center using a Zeiss LSM 510 Meta NLO 2-photon inverted laser scanning microscope equipped with a 40x oil-immersion objective lens. Polyamide–fluorescein conjugates and Mitotracker were imaged in multi-track mode using 488 nm and 543 nm laser excitation with a pinhole of 375 μm and standard filter sets for fluorescein and rhodamine respectively. Hoechst was imaged using 800 nm two-photon excitation with an HFT KP680 dichroic and a 390-465 nm bandpass filter with a fully open pinhole. All images were analyzed using Zeiss LSM software.

Flow Cytometry Analysis.

For flow cytometry experiments A549 cells were plated in 6-well plates at a density of 500 x 10^3 cells per well (133 x 10^3 cells/ml), and allowed to adhere for 16-24 hr before treatment with polyamide-FITC conjugates (100-10,000 nM). Cells were grown for 6, 12, 24, or 48 hr, the medium removed, washed with cold PBS, and trypsinized for 5 min at 37 ° C. The trypsinized cells were combined with the cell culture supernatant and wash solution, and centrifuged for 5 min at 300 x g. This pellet was resuspended, washed with cold PBS, pelleted for 5 min at 300 x g and resuspended in 800 μL Hank's Balanced Salt Solution (2.5 mg/mL BSA, 10 mM HEPES, pH 7.0, no Mg^{2+}, no Ca^{2+}, no phenol red). Cell viability was checked with trypan blue stain and found to be ≥ 90-95% in all cases. Live cells were then diluted to a concentration of 5 x 10^5 cells/mL pipetted through a 40 μm cell strainer (BD Falcon) into 5 mL polystyrene round-bottom tubes (BD Falcon). Just prior to analysis, cells were stained for viability using 7-amino-actinomycin D (7-AAD; eBioscience). Analyses were performed on a BD Bioscience FACSCalibur instrument at the Caltech Flow Cytometry Cell Sorting Facility using standard filter sets for fluorescein and 7-AAD. SPHERO Rainbow Calibration Particles (6 peaks, 3.0-3.4 μm; Spherotech) were used as calibration standards. For each condition 10,000 cells were analyzed. Fluorescence values are representative of the relative median fluorescence (RMF) intensity of the main population, gated for viability based on 7-AAD dye exclusion. Comparison of RMFs of polyamide-labelled cells with SPHERO Rainbow Calibration Particles was used to calculate molecules of equivalent fluorescein per cell, which was converted to a nuclear concentration based on modelling the A549 nucleus as a cylinder with radius 10 μm and height 5 μm to give a calculated nuclear volume of 1 x

10^{-12} L (estimates based on confocal microscopy). All data were analyzed using FlowJo v8.8.2 (TreeStar) and indicate the average and standard deviation of two trials.

Funding

This work was supported by the National Institutes of Health (grant numbers GM51747 and GM27681). J.L.M was supported by a postdoctoral fellowship from the American Cancer Society (grant number PF-10-015-01-CDD). D.C.M. was supported by a National Institutes of Health Cellular, Biochemical, and Molecular Sciences Predoctoral Research training grant (grant number 5T32GM007616).

Acknowledgements

Mass spectrometry analyses were performed in the Mass Spectrometry Laboratory of the Division of Chemistry and Chemical Engineering at the California Institute of Technology. Flow cytometry analyses were performed at the Caltech Flow Cytometry Cell Sorting Facility. We thank Rochelle Diamond for support and technical expertise in performing flow cytometry experiments, and William Dempsey for helpful discussions regarding confocal microscopy.

References

1. Dervan, P. B., Molecular recognition of DNA by small molecules. *Bioorg. Med. Chem.* **2001**, 9, 2215-2235.

2. Dervan, P. B.; Edelson, B. S., Recognition of the DNA minor groove by pyrrole-imidazole polyamides. *Curr. Opin. Struct. Biol.* **2003**, 13, 284-299.

3. Mrksich, M.; Parks, M. E.; Dervan, P. B., Hairpin peptide motif. A new class of oligopeptides for sequence-specific recognition in the minor groove of double-helical DNA. *J. Am. Chem. Soc.* **1994,** 116, 7983-7988.

4. Hsu, C. F., Phillips, J. W., Trauger, J. W., Farkas, M. E., Belitsky, J. M., Heckel, A., Olenyuk, B. Z.; Puckett, J. W.; Wang, C. C.; Dervan, P. B., Completion of a Programmable DNA-Binding Small Molecule Library. *Tetrahedron* **2007,** 63, 6146-6151.

5. Vaquerizas, J. M.; Kummerfeld, S. K.; Teichmann, S. A.; Luscombe, N. M., A census of human transcription factors: function, expression and evolution. *Nat. Rev. Genet.* **2009,** 10, 252-263.

6. Olenyuk, B. Z.; Zhang, G. J.; Klco, J. M.; Nickols, N. G.; Kaelin, W. G.; Jr.; Dervan, P. B., Inhibition of vascular endothelial growth factor with a sequence-specific hypoxia response element antagonist. *Proc. Natl. Acad. Sci. USA* **2004,** 101, 16768-16773.

7. Nickols, N. G.; Dervan, P. B., Suppression of androgen receptor-mediated gene expression by a sequence-specific DNA-binding polyamide. *Proc. Natl. Acad. Sci. USA* **2007,** 104, 10418-10423.

8. Muzikar, K. A.; Nickols, N. G.; Dervan, P. B., Repression of DNA-binding dependent glucocorticoid receptor-mediated gene expression. *Proc. Natl. Acad. Sci. USA* **2009,** 106, 16598-16603.

9. Nickols, N. G.; Jacobs, C. S.; Farkas, M. E.; Dervan, P. B., Modulating hypoxia-inducible transcription by disrupting the HIF-1-DNA interface. *ACS Chem. Biol*. **2007,** 2, 561-571.

10. Matsuda, H.; Fukuda, N.; Ueno, T.; Tahira, Y.; Ayame, H.; Zhang, W.; Bando, T.; Sugiyama, H.; Saito, S.; Matsumoto, K.; Mugishima H.; Serie, K., Development of gene silencing pyrrole-imidazole polyamide targeting the TGF-beta1 promoter for treatment of progressive renal diseases. *J. Am. Soc. Nephrol.* **2006,** 17, 422-432.

11. Best, T. P.; Edelson, B. S.; Nickols, N. G.; Dervan, P. B., Nuclear localization of pyrrole-imidazole polyamide-fluorescein conjugates in cell culture. *Proc. Natl. Acad. Sci. USA* **2003,** 100, 12063-12068.

12. Edelson, B. S.; Best, T. P.; Olenyuk, B.; Nickols, N. G.; Doss, R. M.; Foister, S.; Heckel, A.; Dervan, P. B., Influence of structural variation on nuclear localization of DNA-binding polyamide-fluorophore conjugates. *Nucleic Acids Res*. **2004,** 32, 2802-2818.

13. Jacobs, C. S.; Dervan, P. B., Modifications at the C-terminus to improve pyrrole-imidazole polyamide activity in cell culture. *J. Med. Chem.* **2009,** 52, 7380-7388.

14. Nishijima, S.; Shinohara, K.; Bando, T.; Minoshima, M.; Kashiwazaki, G.; Sugiyama, H., Cell permeability of Py-Im-polyamide-fluorescein conjugates: Influence of molecular size and Py/Im content. *Bioorg. Med. Chem.* **2010,** 18, 978-983.

15. Nickols, N. G.; Jacobs, C. S.; Farkas, M. E.; Dervan, P. B., Improved nuclear localization of DNA-binding polyamides. *Nucleic Acids Res.* **2007,** 35, 363-370.

16. Herman, D. M.; Baird, E. E.; Dervan, P. B., Stereochemical control of the DNA binding affinity, sequence specificity, and orientation preference of chiral hairpin polyamides in the minor groove. *J. Am. Chem. Soc.* **1998,** 120, 1382-1391.

17. Chenoweth, D. M.; Dervan, P. B., Allosteric modulation of DNA by small molecules. *Proc. Natl. Acad. Sci. USA* **2009,** 106, 13175-13179.

18. Chenoweth, D. M.; Harki, D. A.; Phillips, J. W.; Dose, C.; Dervan, P. B., Cyclic pyrrole-imidazole polyamides targeted to the androgen response element. *J. Am. Chem. Soc.* **2009,** 131, 7182-7188.

19. Belitsky, J. M.; Nguyen, D. H.; Wurtz, N. R.; Dervan, P. B., Solid-phase synthesis of DNA binding polyamides on oxime resin. *Bioorg. Med. Chem.* **2002,** 10, 2767-2774.

20. Krutzik, P. O.; Chamberlin, A. R., Synthesis of DNA-binding polyamides. Robust solid-phase methods for coupling heterocyclic aromatic amino acids. *Methods Mol. Biol.* **2002,** 201, 77-92.

21. Dose, C.; Farkas, M. E.; Chenoweth, D. M.; Dervan, P. B., Next generation hairpin polyamides with (R)-3,4-diaminobutyric acid turn unit. *J. Am. Chem. Soc.* **2008,** 130, 6859-6866.

22. Vichai, V.; Kirtikara, K., Sulforhodamine B colorimetric assay for cytotoxicity screening. *Nat. Protoc.* **2006,** 1, 1112-1116.

23. So, A. Y.; Chaivorapol, C.; Bolton, E. C.; Li, H.; Yamamoto, K. R., Determinants of cell- and gene-specific transcriptional regulation by the glucocorticoid receptor. *PLoS Genet.* **2007,** 3, e94.

24. Reddy, T. E.; Pauli, F.; Sprouse, R. O.; Neff, N. F.; Newberry, K. M.; Garabedian, M. J.; Myers, R. M., Genomic determination of the glucocorticoid response reveals unexpected mechanisms of gene regulation. *Genome Res.* **2009,** 19, 2163-2171.

25. Meijsing, S. H.; Pufall, M. A.; So, A. Y.; Bates, D. L.; Chen, L.; Yamamoto, K. R., DNA binding site sequence directs glucocorticoid receptor structure and activity. *Science* **2009,** 324, 407-410.

26. Hsu, C. F.; Dervan, P. B., Quantitating the concentration of Py-Im polyamide-fluorescein conjugates in live cells. *Bioorg. Med. Chem. Lett.* **2008,** 18, 5851-5855.

27. Crowley, K. S.; Phillion, D. P.; Woodard, S. S.; Schweitzer, B. A.; Singh, M.; Shabany, H.; Burnette, B.; Hippenmeyer, P.; Heitmeier, M.; Bashkin, J. K., Controlling the intracellular localization of fluorescent polyamide analogues in cultured cells. *Bioorg. Med. Chem. Lett.* **2003,** 13, 1565-1570.

28. Dickinson, L. A.; Burnett, R.; Melander, C.; Edelson, B. S.; Arora, P. S.; Dervan, P. B.; Gottesfeld, J. M., Arresting cancer proliferation by small-molecule gene regulation. *Chem. Biol.* **2004,** 11, 1583-1594.

29. Tsai, S. M.; Farkas, M. E.; Chou, C. J.; Gottesfeld, J. M.; Dervan, P. B., Unanticipated differences between alpha- and gamma-diaminobutyric acid-linked hairpin polyamide-alkylator conjugates. *Nucleic Acids Res.* **2007,** 35, 307-316.

30. Rucker, V. C.; Foister, S.; Melander, C.; Dervan, P. B., Sequence specific fluorescence detection of double strand DNA. *J. Am. Chem. Soc.* **2003,** 125, 1195-1202.

31. Bradford, J. A.; Clarke, S. T., Dual-pulse labeling using 5-ethynyl-2'-deoxyuridine (EdU) and 5-bromo-2'-deoxyuridine (BrdU) in flow cytometry. *Curr. Protoc. Cytom.* **2011,** 55, 7.38.1–7.38.15.

32. Poulin-Kerstien, A. T.; Dervan, P. B., DNA-templated dimerization of hairpin polyamides. *J. Am. Chem. Soc.* **2003,** 125, 15811-15821.

33. Gissot, A.; Camplo, M.; Grinstaff, M. W.; Barthelemy, P., Nucleoside, nucleotide and oligonucleotide based amphiphiles: a successful marriage of nucleic acids with lipids. *Org. Biomol. Chem.* **2008,** 6, 1324-1333.

34. Bijsterbosch, M. K.; Rump, E. T.; De Vrueh, R. L.; Dorland, R.; van Veghel, R.; Tivel, K. L.; Biessen, E. A.; van Berkel, T. J.; Manoharan, M., Modulation of plasma protein binding and in vivo liver cell uptake of phosphorothioate oligodeoxynucleotides by cholesterol conjugation. *Nucleic Acids Res.* **2000,** 28, 2717-2725.

35. Van Dyke, M. W.; Hertzberg, R. P.; Dervan, P. B., Map of distamycin, netropsin, and actinomycin binding sites on heterogeneous DNA: DNA cleavage-inhibition patterns with methidiumpropyl-EDTA·Fe(II). *Proc. Natl. Acad. Sci. USA* **1982,** 79, 5470-5474.

36. Schultz, P. G.; Taylor, J. S.; Dervan, P. B., Design and Synthesis of a Sequence-Specific DNA Cleaving Molecule. (Distamycin-EDTA)iron(II). *J. Am. Chem. Soc.* **1982,** 104, 6861-6863.

37. Schmidt, T. L.; Heckel, A., Pyrrole/imidazole-polyamide anchors for DNA tertiary interactions. *Small* **2009,** 5, 1517-1520.

38. Cohen, J. D.; Sadowski, J. P.; Dervan, P. B., Programming multiple protein patterns on a single DNA nanostructure. *J. Am. Chem. Soc.* **2008,** 130, 402-403.

39. Johnson, D. S.; Mortazavi, A.; Myers, R. M.; Wold, B., Genome-wide mapping of in vivo protein-DNA interactions. *Science* **2007,** 316, 1497-1502.

40. Hesselberth, J. R.; Chen, X.; Zhang, Z.; Sabo, P. J.; Sandstrom, R.; Reynolds, A. P.; Thurman, R. E.; Neph, S.; Kuehn, M. S.; Noble, W. S.; Fields, S.; Stamatoyannopoulos, J. A., Global mapping of protein-DNA interactions in vivo by digital genomic footprinting. *Nat. Methods* **2009,** 6, 283-289.

41. Ohtsukia, A.; Kimurab, M. T.; Minoshimaa, M.; Suzukib, T.; Ikedab, M.; Bandoa, T.; Nagase, H.; Shinohara, K.; Sugiyama, H., Synthesis and properties of PI polyamide–SAHA conjugate. *Tetrahedron Lett.* **2009,** 50, 7288-7292.

42. Kwon, Y.; Arndt, H. D.; Mao, Q.; Choi, Y.; Kawazoe, Y.; Dervan, P. B.; Uesugi, M., Small molecule transcription factor mimic. *J. Am. Chem. Soc.* **2004,** 126, 15940-15941.

43. Mapp, A. K.; Ansari, A. Z.; Ptashne, M.; Dervan, P. B., Activation of gene expression by small molecule transcription factors. *Proc. Natl. Acad. Sci. USA* **2000,** 97, 3930-3935.

44. Baird, E. E.; Dervan, P. B., Solid phase synthesis of polyamides containing imidazole and pyrrole amino acids. *J. Am. Chem. Soc.* **1996,** 118, 6141-6146.

45. Chenoweth, D. M.; Harki, D. A.; Dervan, P. B., Solution-phase synthesis of pyrrole-imidazole polyamides. *J. Am. Chem. Soc.* **2009,** 131, 7175-7181.

46. Krutzik, P. O.; Chamberlin, A. R., Synthesis of DNA-binding polyamides. Robust solid-phase methods for coupling heterocyclic aromatic amino acids. *Methods Mol. Biol.* **2002,** 201, 77-92.